AD-A144 122 ADVANCED STUDIES OF INTEGRABLE SYSTEMS(U) CLARKSON COLL OF TECHNOLOGY POTSDAM N Y DEPT OF PHYSICS D J KAUP 26 JUN 84 AFOSR-TR-84-0593 AFOSR-82-0154 1/1

UNCLASSIFIED F/G 21/2 NL

END
DATE
FILMED
9 84
DTIC

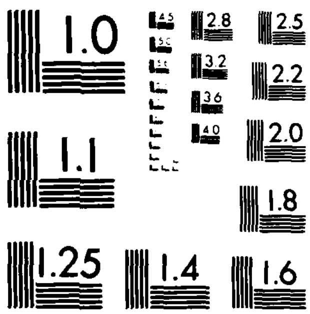

MICROCOPY RESOLUTION TEST CHART
NATIONAL BUREAU OF STANDARDS 1963 A

AFOSR-TR- 84-0593

(4)

AD-A144 122

INTERIM TECHNICAL REPORT

FOR PERIOD ENDING 5/31/84

ADVANCED STUDIES OF INTEGRABLE SYSTEMS

Contract No. AFOSR-82-0154

by

David J. Kaup
Professor of Physics
Clarkson University
Potsdam, NY 13676

DTIC FILE COPY

DTIC
ELECTE
AUG 8 1984
S D
D

Approved for public release;
distribution unlimited.

84 08 07 110

UNCLASSIFIED
SECURITY CLASSIFICATION OF THIS PAGE

REPORT DOCUMENTATION PAGE

1a. REPORT SECURITY CLASSIFICATION UNCLASSIFIED	1b. RESTRICTIVE MARKINGS
2a. SECURITY CLASSIFICATION AUTHORITY	3. DISTRIBUTION/AVAILABILITY OF REPORT Approved for public release; distribution unlimited.
2b. DECLASSIFICATION/DOWNGRADING SCHEDULE	
4. PERFORMING ORGANIZATION REPORT NUMBER(S)	5. MONITORING ORGANIZATION REPORT NUMBER(S) AFOSR-TR- 84-0593
6a. NAME OF PERFORMING ORGANIZATION Clarkson College / 6b. OFFICE SYMBOL (If applicable)	7a. NAME OF MONITORING ORGANIZATION Air Force Office of Scientific Research
6c. ADDRESS (City, State and ZIP Code) Department of Physics Potsdam NY 13676	7b. ADDRESS (City, State and ZIP Code) Directorate of Mathematical & Information Sciences, Bolling AFB DC 20332
8a. NAME OF FUNDING/SPONSORING ORGANIZATION AFOSR / 8b. OFFICE SYMBOL (If applicable) NM	9. PROCUREMENT INSTRUMENT IDENTIFICATION NUMBER AFOSR-82-0154
8c. ADDRESS (City, State and ZIP Code) Bolling AFB DC 20332	10. SOURCE OF FUNDING NOS. PROGRAM ELEMENT NO.: 61102F; PROJECT NO.: 2304; TASK NO.: A4; WORK UNIT NO.:
11. TITLE (Include Security Classification) ADVANCED STUDIES OF INTEGRABLE SYSTEMS	
12. PERSONAL AUTHOR(S) David J. Kaup	
13a. TYPE OF REPORT Interim / 13b. TIME COVERED FROM 1/6/83 TO 31/5/84	14. DATE OF REPORT (Yr., Mo., Day) 26 JUN 84 / 15. PAGE COUNT 3
16. SUPPLEMENTARY NOTATION	
17. COSATI CODES FIELD / GROUP / SUB. GR.	18. SUBJECT TERMS (Continue on reverse if necessary and identify by block number)

19. ABSTRACT (Continue on reverse if necessary and identify by block number)

A scientific report is presented covering publications resulting from a one year study of advanced topics in integrable systems. These publications cover studies on: Soliton Dynamics in the Presence of External Forces; Nonlinear Scattering of Whistlers by Electro-Static Fluctuations; The Force Toda Lattice: An example of an almost integrable system; The Soliton Birth Rate in the Forced Toda Lattice; and Whistler Scattering From Density Fluctuations in Magnetized Plasmas.

20. DISTRIBUTION/AVAILABILITY OF ABSTRACT UNCLASSIFIED/UNLIMITED ☒ SAME AS RPT. ☐ DTIC USERS ☐	21. ABSTRACT SECURITY CLASSIFICATION UNCLASSIFIED
22a. NAME OF RESPONSIBLE INDIVIDUAL Dr. Robert N. Buchal	22b. TELEPHONE NUMBER (Include Area Code) (202) 767- 4939 / 22c. OFFICE SYMBOL NM

DD FORM 1473, 83 APR EDITION OF 1 JAN 73 IS OBSOLETE.

UNCLASSIFIED
SECURITY CLASSIFICATION OF THIS PAGE

TABLE OF CONTENTS

TECHNICAL REPORT

Accession For
NTIS GRA&I ☒
DTIC TAB ☐
Unannounced ☐
Justification

By
Distribution/
Availability Codes
Dist | Avail and/or Special
A/1

COPY INSPECTED

AIR FORCE
NOTICE
This
MATTHEW J.
Chief, Technical Information Division

I. TECHNICAL REPORT

A. Soliton Dynamics in the Presence of External Forces
[Phys. Rev. B 29, 1072-4 (1984)] (Reprint enclosed)

In this paper, a recent conjecture that solitons are not "newtonian particles" is discussed. It is shown that whether or not newtonian motion is observed will depend critically on the definition of the soliton's center.

B. Nonlinear Scattering of Whistlers by Electrostatic Fluctuations
[Phys. Rev. A 29, 396-8 (1984)] (coauthored by P.K. Shukla, M.Y. Yu and S.N. Antani; reprint enclosed)

Sharply localized distributions of whistler waves have been observed in the ionosphere and the solar wind. In this paper it is demonstrated that such distributions could possibly be explained by a modulational instability arising from interactions with ion-cyclotron waves.

C. The Forced Toda Lattice: An example of an almost integrable system
[J.Math.Phys. 25, 277-81 (1984)] (Reprint enclosed)

In this paper, I discuss forced integrable systems using the forced Toda lattice as an example. I also demonstrate how these systems are 'almost integrable'.

D. The Soliton Birth Rate in the Forced Toda Lattice
[J.Math.Phys. 25, 282-4 (1984)] (co-authored with D.H. Neuberger; Reprint enclosed)

The numerical analysis of the forced Toda lattice allowed us to demonstrate that one could quite easily predict the soliton birth rate in this system.

E. Whistler Scattering from Density Fluctuations in Magnetized Plasmas
[Phys. Fluids 27, 1169-75 (1984)] (coauthored with S.N. Antani; reprint enclosed)

The nonlinear interactions of whistler waves with density fluctuations in magnetized plasmas is studied. It is found that this will be a major interaction in proposed commercial Tokamaks, and that instead of nonlinearities dominating, the diffusion effects would dominate with a subsequent loss in the coherence of any such whistler beam.

Comment on "Specific sine-Gordon soliton dynamics in the presence of external driving forces"

D. J. Kaup
Nonlinear Studies Institute, Clarkson College of Technology, Potsdam, New York 13676
(Received 27 September 1982)

It is shown that the results presented by Reinisch and Fernandez have an alternative interpretation where the soliton does behave as a Newtonian particle. The key features required for this alternative interpretation are (i) properly defining where the center of the soliton is, and (ii) expanding the solution so as to avoid any secular terms. When these two objectives are achieved, then the center of the soliton is found to satisfy Newton's equation of motion for a point particle.

Recently there has been some controversy about the validity of soliton perturbation theories and the interpretation of a soliton as a particle. This was first noted in Ko and Kuehl's[1] study of the $K\,dV$ equation with time-dependent coefficients. Their result for the position of a soliton x_m, when transformed into the notation of Kaup and Newell,[2] gave

$$\frac{dx_m}{dt}=4\eta^2-\frac{\Gamma}{3\eta} ,$$

where $2\eta^2$ is the amplitude of the soliton and Γ is the damping. On the other hand, a soliton perturbation theory found[2]

$$\frac{d\bar{x}}{dt}=4\eta^2+\frac{\Gamma}{3\eta} ,$$

where $\bar{x}$ is Kaup and Newell's position for the soliton. These sign differences are real, and numerical results did support Ko and Kuehl's result.[3]

More recently Reinisch and Fernandez have numerically studied[4] the sine-Gordon kink under the influence of a constant torque. They also found their numerical results at variance with the predictions of soliton perturbation theories[5–10] and have proposed to explain this by declaring the soliton to be a *non*-Newtonian particle. What I propose is that one does not have to be that drastic and also that the Ko and Kuehl observation and the Reinisch and Fernandez observation may have a common explanation.

First, let me state some facts, then I shall give my interpretation of these results.

(1) The soliton or kink is *not* rigid and is *not* a "point particle."[11] (Therefore one must qualify to what extent one is referring to it as a "Newtonian" or a "non-Newtonian" particle. Should one look at the short-time or long-time scales to see this?)

(2) Any "extended particle" will respond with a time delay to an externally applied force.[12] (This is also verified by Reinisch and Fernandez's numerical results. To the extent that the soliton is not a point particle, one could say that the soliton was non-Newtonian. In this respect, Reinisch and Fernandez were correct. What they observed were the combined transient effects of a soliton reshaping itself[11] and experiencing a time delay.)

(3) The expansion used by Reinisch and Fernandez contained secular terms. (The presence of secular terms limits the validity of their expansion to short-time scales.)

(4) The concept of a "soliton" comes from considering the solution for $t\to+\infty$, whereby the general solution separates into "a collection of solitons in a sea of radiation." (Thus to identify or locate a soliton, one should use a solution valid for *large*-time scales, not short-time scales.)

(5) The definition of the center of a soliton used by Reinisch and Fernandez is different from the definition used in soliton perturbation theories.

Now what I want to do here is to present an alternative interpretation of the Reinisch and Fernandez result.[4] As they did, I start with the perturbed sine-Gordon equation

$$u_{tt}-u_{xx}+\sin u=\epsilon R(x,t) . \tag{1}$$

I now difffer from their procedure and instead expand u as

$$u(x,t)=U_0(\chi)+\epsilon u^{(1)}(\chi,t)+\dots , \tag{2}$$

where χ is to be determined and $U_0(\chi)$ is exactly the one-soliton soliton given by

$$U_0(\chi)=4\tan^{-1}(e^{\pm\chi}) . \tag{3}$$

χ shall be defined such that no secular terms will appear in (2). I shall define the center of the soliton to be at the center of U_0, which is where $\chi=0$. This also differs from the definition of the center according to Reinisch and Fernandez, who took it to be where $u_x(x,t)$ was a maximum. To avoid relativistic effects and to maintain simplicity, I shall take $\chi_t\le O(\epsilon)$, and require that

$$\chi_x^2=1+\chi_t^2 . \tag{4}$$

Then from (1), (2), and (4), the first-order result is

$$U_{0\chi}\chi_{tt}+\epsilon u_{tt}^{(1)}+\epsilon L u^{(1)}=\epsilon R , \tag{5}$$

where

$$L=-\partial_\chi^2+\cos U_0(\chi) . \tag{6}$$

The operator L has one zero eigenvalue, which is a bound state whose eigenfunction is proportional to $U_{0\chi}$.[7] If I now demand that $u^{(1)}$ must not contain any secular terms in this (first) order, then $u^{(11)}$ must be orthogonal to this bound-state eigenfunction. Thus I take

$$u^{(1)}(\chi,t)=\int_{-\infty}^{\infty}dk\, a_k(t)f_k(\chi) , \tag{7}$$

whence both χ and a_k are uniquely determined by

$$\chi_{tt}=\epsilon\frac{\int_{-\infty}^{\infty}f_b(\chi)R(x,t)d\chi}{\int_{-\infty}^{\infty}f_b(\chi)U_{0\chi}(\chi)d\chi} , \tag{8}$$

 ©1984 The American Physical Society

and

$$a_{ktt} + \omega_k^2 a_k = \int_{-\infty}^{\infty} f_k(X) R(x,t)\, dX \quad . \tag{9}$$

In the above, f_b and f_k are the eigenfunctions of L (Ref. 7) and $\omega_k^2 = 1 + k^2$. Equations (8) and (9) are the results for a general forcing term $R(x,t)$. As one may see from (8), the acceleration X_{tt} of the soliton is directly proportional to the bound-state component of $R(x,t)$, while from (9), the amplitude of the continuous spectrum is driven by the kth component of $R(x,t)$.

Now, as in Ref. 4, let us take R independent of x, so that we have a constant torque being applied to the sine-Gordon field. Also, take $R = 0$ if $t < 0$ and R constant for $t > 0$. Then for $t > 0$, (8) yields

$$X_{tt} = \pm \epsilon \frac{\pi}{4} R \quad , \tag{10}$$

from which we obtain

$$X = x \pm \frac{\pi}{4} \epsilon R \frac{t^2}{2} \quad . \tag{11}$$

Since the center of the soliton is at $X = 0$, it then follows that the soliton (our definition of the center at least) does behave as a Newtonian particle.[2,5–11]

However, as was indeed pointed out in Ref. 4, *such is not observed.* And to understand what has occurred in these numerical experiments,[4] we must include the effects of the continuous spectrum. From (9), one can readily obtain[4,7]

$$u^{(1)}(X,t) + -\frac{\epsilon}{2} R \int_{-\infty}^{\infty} dk\, G(k,X)[1 - \cos(\omega_k t)] \quad , \tag{12}$$

where

$$G(k,X) = \frac{k\cos(kX) - \sin(kX)\tanh X}{(1+k^2)^2 \sinh(\pi k/2)} \quad . \tag{13}$$

In Ref. 4, the integral in (12) is evaluated by contour integration and is reduced to an infinite series. However, that infinite series is only convergent if one is *outside* the light cone. Inside the light cone, one must use other techniques. For large times $u^{(1)}$ will conveniently separate into the two parts

$$u^{(1)} = -\frac{\epsilon}{2} R \int_{-\infty}^{\infty} dk\, G(k,X) + \frac{\epsilon}{2} R \int_{-\infty}^{\infty} dk\, G(k,X) \cos(\omega_k t) \quad . \tag{14}$$

The first part is time independent, and corresponds to a permanent change in the soliton's shape. The second term may be evaluated by stationary phase, and represents outward traveling radiation.

If instead we are interested in short-time scales, then we may expand (12) in a Taylor series, obtaining

$$u^{(1)}(X,t) = -\frac{\epsilon}{4} R t^2 \int_{-\infty}^{\infty} dk\,(1+k^2) G(k,X) + O(t^4) \quad , \tag{15}$$

which evaluates to

$$u^{(1)}(X,t) = \frac{\epsilon t^2}{4} R \left(2 - \frac{\pi}{\cosh X} \right) + \cdots \quad . \tag{16}$$

Now from (2), (11), and (16), we have

$$u(x,t) = U_0\left(x \pm \frac{\pi}{8} \epsilon R t^2 \right) + \frac{\epsilon t^2}{4} R \left(2 - \frac{\pi}{\cosh X} \right) + O(t^4) \quad . \tag{17}$$

Since we have evaluated (12) by a Taylor's series expansion in t, we may as well do the same for the soliton part, noting that $U_{0X} = \pm 2/\cosh X$. Whence

$$u(x,t) = U_0(x) + \tfrac{1}{2} \epsilon t^2 R + O(t^4) \quad . \tag{18}$$

Naturally, Eq. (18) is exactly the same result as that obtained in Ref. 4. However, I have obtained it via a different definition and interpretation. I interpret Eq. (17) as a Newtonian particle moving with a constant acceleration, and with radiation being created at a rate proportional to t^2 on short-time scales. What will be observed numerically is shown in Eq. (18). As shown by Eq. (18), the buildup of the above-created radiation will exactly cancel the soliton motion, causing the soliton to seem to hang motionless.

One can also explain this by considering the various time scale involved. In a Taylor series expansion as in Eq. (18), one is implicitly considering the response of the system on a very-short-time scale, at least faster than the time required for a signal to cross the width of the soliton. On such a short-time scale, for example, the left side of the soliton will not know what has happened on the right side of the soliton. Thus whatever happens on the right side cannot effect the left side. Thus each element of the sine-Gordon field will respond *independently* of all other elements. To make this clearer, consider now Eq. (1) on this short-time scale, and in the rest frame of the soliton. Since we start with an equilibrium state, we have $u_{xx} - \sin u = 0$, at least on this time scale, which leaves only

$$u_{tt} = \epsilon R(x,t) \quad . \tag{19}$$

What (19) demonstrates is simply that the response of u at x is independent of what u is at another value of x. Each element of u is responding like a free particle, independent of all other elements, and its response is only determined by the value of the forcing term at the position of that element. In other words, the concepts of solitons and radiation are only of value when one is concerned with or interested in the intermediate or long-time behavior. On the short-time scales, the soliton concept is of less value than the field concept, as was demonstrated by Eq. (19).

I also suggest that a similar analysis of the $K\,dV$ equation may well explain Ko and Kuehl's[1] result, but that remains to be seen.

[1]K. Ko and H. H. Kuehl, Phys. Rev. Lett. 40, 233 (1978).
[2]D. J. Kaup and A. C. Newell, Proc. R. Soc. London, Ser. A 361, 413 (1978).
[3]H. H. Kuehl (private communication).
[4]G. Reinisch and J. C. Fernandez, Phys. Rev. B 24, 835 (1981).
[5]D. J. Kaup, SIAM J. Appl. Math. 31, 121 (1976).
[6]J. P. Keener and D. W. McLaughlin, Phys. Rev. A 16, 777 (1977); J. Math. Phys. 18, 2008 (1977).
[7]A. R. Bishop, J. A. Krumhansl, and S. E. Trullinger, Physica D 1, 1 (1980).
[8]D. W. McLaughlin and A. C. Scott, Phys. Rev. A 18, 1652 (1978).
[9]*Solitons in Action*, edited by K. Lonngren and A. C. Scott (Academic, New York, 1978).
[10]*Solitons*, edited by R. K. Bullough and P. J. Caudrey (Springer, New York, 1980).
[11]M. B. Fogel, S. E. Trullinger, A. R. Bishop, and J. A. Krumhansl, Phys. Rev. B 15, 1578 (1977).
[12]D. J. Kaup, Phys. Rev. 152, 1130 (1966), and references therein.

Nonlinear scattering of whistlers by electrostatic fluctuations

P. K. Shukla and M. Y. Yu
Institut für Theoretische Physik I, Ruhr-Universität Bochum, D-4630 Bochum 1, Federal Republic of Germany

S. N. Antani* and D. J. Kaup
Department of Physics, Clarkson College of Technology, Potsdam, New York 13676

(Received 28 October 1982; revised manuscript received 29 March 1983)

It is found that nonlinear coupling of whistler waves with ion-cyclotron fluctuations can lead to spiky whistler electric field envelopes. Analytical results for the latter, which are solutions with discontinuous derivatives, are given. Possible application of our results in solar-wind plasmas is discussed.

The knowledge of nonlinear propagation of electron whistler waves is very essential to the understanding of wave phenomena in both ionosphere and space physics.[1] In particular, nonlinear interaction of whistlers with adiabatic particle motion, ion-acoustic oscillations, and magnetohydrodynamic perturbations can lead to the modulational instabilities.[2,3] The latter can give rise to self-focusing, wave localization, and soliton formation.[3,4]

In this paper we consider the interaction of whistlers with electrostatic ion-cyclotron oscillations. It is found that such an interaction produces spiky whistler envelope solitions. Analytical results for the latter are given, and application to space plasma is discussed.

Consider the propagation of right-handed circularly polarized whistler waves in the form

$$\vec{E}=E(\hat{x}+i\hat{y})\exp(i\vec{k}\cdot\vec{x}-i\omega t)+\text{c.c.} \tag{1}$$

The frequency ω and the wave number $\vec{k}$ are related by the dispersion relation

$$\frac{c^2k^2}{\omega^2}=1+\frac{\omega_{pe}^2}{\omega(\Omega_e\cos\theta-\omega)} , \tag{2}$$

where $\cos\theta=k_z/k$, $k^2=k_\perp^2+k_z^2$; ω_{pe} and Ω_e are the electron plasma and gyrofrequencies, respectively. The cold plasma dispersion relation given above is valid for $|\omega-\Omega_e|>>k_zv_{te}$, $\omega>>\Omega_i$, and $\omega>\omega_{pi}/(1+\omega_{pe}^2/\Omega_e^2)^{1/2}$, where v_{te} is the electron thermal velocity; Ω_i and ω_{pi} are the ion gyro and plasma frequencies, respectively.

Nonlinear interaction of whistler waves propagating along the external magnetic field $B_0\hat{z}$ with slow background plasma motion gives rise to an envelope of waves governed by the nonlinear Schrödinger equation[3,4]

$$i(\partial_t+v_g\partial_z)E+\tfrac{1}{2}v_g'\partial_z^2E+\tfrac{1}{2}T\partial_x^2E-\Delta E=0 , \tag{3}$$

where $v_g=2\omega(\Omega_e-\omega)/k\Omega_e$ is the group velocity, $v_g'=v_g\times(\Omega_e-4\omega)/k\Omega_e$, and $T=v_g(\Omega_e-2\omega)/2k(\Omega_e-\omega)$ are the parallel (to $\vec{B}_0$) and perpendicular group dispersions, respectively.

The nonlinear frequency shift Δ appearing in (3) is given by

$$\Delta\approx-\frac{kv_g}{2}\left[\frac{\delta n}{n_0}-\frac{2v_z}{v_g}\right] , \tag{4}$$

where n_0 is the unperturbed density, and we have assumed $\omega_{pe}^2>>\omega(\Omega_e-\omega)$. Note that $\vec{k}\parallel\hat{z}$, but the slow modulation is in both x and z directions. Here, δn and v_z are the electron density and field aligned velocity perturbations associated with the low-frequency plasma motion. The two are related by the electron continuity equation

$$\partial_t\delta n+n_0\partial_zv_z=0 , \tag{5}$$

where, in view of the low frequency ($\partial_t<<\Omega_e$), we have used the drift approximation $\vec{v}_\perp=\vec{v}_E=c\hat{z}\times\vec{\nabla}_\perp\phi/B_0$, where ϕ is the slow ambipolar potential. Note that $\vec{\nabla}\cdot\vec{v}_E=0$, and that there are no density perturbations associated with the whistler waves.

We shall limit to electrostatic low-frequency response, and let the parallel phase velocity of the modulation be much smaller than the electron thermal velocity. The slow electrons are then in equilibrium along $\vec{B}_0$. From the parallel momentum equation, one then obtains the corresponding electron density perturbations[3]

$$\partial_z\delta n/n_0=\partial_z\Phi+F , \tag{6}$$

where $\Phi=e\phi/T_e$, T_e being the electron temperature. Here, F represents the low-frequency ponderomotive force due to the whistler fields; it is given by[3,5]

$$F=\frac{\omega_{pe}^2}{\omega(\Omega_e-\omega)}\left[\partial_z+\frac{2}{v_g}\partial_t\right]\frac{|E|^2}{16\pi n_0T_e} . \tag{7}$$

Under the quasineutrality condition, the slow ion motion is given by

$$\partial_t\delta n+n_0\vec{\nabla}_\perp\cdot\vec{v}_{i\perp}+n_0\partial_zv_{iz}=0 , \tag{8}$$

$$\partial_t\vec{v}_{i\perp}=-c_s^2\vec{\nabla}_\perp\Phi+\Omega_i\vec{v}_{i\perp}\times\hat{z}-v_{ti}^2\vec{\nabla}_\perp\delta n/n_0 , \tag{9}$$

$$\partial_tv_{iz}=-c_s^2\partial_z\Phi-v_{ti}^2\partial_z\delta n/n_0 . \tag{10}$$

where $c_s=(T_e/m_i)^{1/2}$ and $v_{ti}=(\gamma T_i/m_i)^{1/2}$ are the ion sound and ion thermal velocities, respectively. The effect of the ponderomotive force on the ions is negligible since the whistler waves do not involve ion motion.

Although according to these equations the ion motion is linear, its nonlinear coupling to the whistler waves occurs through the ambipolar potential Φ appearing in (6). From

 ©1984 The American Physical Society

(9) we get

$$(\partial_t^2+\Omega_i^2)\vec{v}_{i\perp}=-c_s^2\partial_t\vec{\nabla}_\perp\Phi-\Omega_i c_s^2\vec{\nabla}_\perp\Phi\times\hat{z}-v_{ti}^2\partial_t\vec{\nabla}_\perp\delta n/n_0\ . \quad (11)$$

Combining (8), (10), and (11), we find

$$[\partial_t^2(\partial_t^2+\Omega_i^2)-v_{ti}^2\nabla^2\partial_t^2-\Omega_i^2v_{ti}^2\partial_z^2]\delta n/n_0=c_s^2(\nabla^2\partial_t^2+\Omega_i^2\partial_z^2)\Phi\ , \quad (12)$$

where $\nabla^2=\nabla_\perp^2+\partial_z^2$. Eliminating Φ from (6) and (12), we obtain

$$[\partial_t^2(\partial_t^2+\Omega_i^2)-c_a^2\nabla^2\partial_t^2-\Omega_i^2c_a^2\partial_z^2]\partial_z\delta n/n_0=-c_s^2(\nabla^2\partial_t^2+\Omega_i^2\partial_z^2)F\ , \quad (13)$$

where $c_a^2=(\gamma T_i+T_e)/m_i$.

Equation (13) describes four types of driven low-frequency, electrostatic oscillations. First, for $\partial_t\to 0$ (adiabatic response),[4] we obtain from (13) that $v_z=0$, and

$$\partial_z(\delta n/n_0)=[T_e/(T_e+T_i)]F\ , \quad (14)$$

where F is given by (7) with $\partial_t=0$. This modulation leads to a positive density perturbation for $\omega<\Omega_e$. One can easily show that the usual hyperbolic-secant-profile standing envelope solitons exist if $\omega<\Omega_e/4$ (i.e., $v_g'>0$).

For $\partial_t<<\Omega_i$, $\nabla_\perp^2<<\partial_z^2$, and $\Omega_i^{-2}c_a^2\nabla_\perp^2<<1$, Eq. (13) yields the driven slow ion-acoustic oscillations, namely,[4]

$$(\partial_t^2-c_a^2\partial_z^2)\partial_z\delta n/n_0=-c_s^2\partial_z^2F\ . \quad (15)$$

For this case, one can show that sub- as well as supersonic hyperbolic-secant-profile solitons exist.[4]

For $\Omega_i<<\partial_t$ and $\partial_z^2<<\nabla_\perp^2$, one obtains the driven fast ion-acoustic waves, moving predominantly across the external magnetic field.

In this paper, we are interested in investigating the nonlinear state involving the whistlers and the ion-cyclotron fluctuations. The latter satisfy $\partial_t\sim\Omega_i$ and $\partial_z^2<<\nabla_\perp^2$. Thus we obtain from (13)

$$(\partial_t^2+\Omega_i^2-c_a^2\nabla_\perp^2)\partial_z\delta n/n_0=-c_s^2\partial_z^2F\ , \quad (16)$$

which gives the ion-cyclotron wave response in the presence of the ponderomotive force.

We look for stationary solutions of the coupled set (3), (5), and (16). We let

$$E=W(\xi)\exp(i\delta t)\ , \quad (17)$$

where W and δ are real, and $\xi=x+\alpha z-Vt$. The constants α and V are real, and for the present modulation $\alpha<<1$.

For localized perturbations, we require $v_z(\xi)$, $\delta n(\xi)$, and $W(\xi)\to 0$ for $|\xi|\to\infty$. One obtains from (5) and (16) $v_z=v_p\delta n/n_0$ and

$$\delta n/n_0=-\rho_s^2(1-2v_p/v_g)\partial_\xi^2\mathcal{E}^2\ , \quad (18)$$

where $\mathcal{E}^2=W^2/16\pi n_0T_e$, $v_p=V/\alpha$, and $\rho_s=c_s/\Omega_i$. Combining (4) and (18), we get $\Delta=Q\partial_\xi^2\mathcal{E}^2$, where

$$Q=\tfrac{1}{2}kv_g(1-2v_p/v_g)^2\rho_s^2\ . \quad (19)$$

The wave equation (3) then yields $V=\alpha v_g$, and

$$\tfrac{1}{2}P\partial_\xi^2\mathcal{E}-\delta\mathcal{E}-Q\mathcal{E}\partial_\xi^2\mathcal{E}^2=0\ , \quad (20)$$

where $P=\alpha^2v_g'+T$. Equation (20), which contains a derivative in the nonlinear term, is similar to that describing upper-hybrid solitons.[6] It has a localized solution given by the relation

$$\mathcal{E}=\mathcal{E}_0\mathrm{sech}[(x+\alpha z-Vt)/L+(1-\mathcal{E}^2/\mathcal{E}_0^2)^{1/2}]\ , \quad (21)$$

where $\mathcal{E}^2=P/4Q$ and $L^2=P/2\delta$. Note that $\delta>0$, $P>0$, and $\alpha<<1$ are necessary for the existence of the soliton. Furthermore, we note that the function $\mathcal{E}$ also appears in the argument of the hyperbolic-secant function, and that the theory breaks down if $2v_p=v_g$. The slope of the soliton electric field $\mathcal{E}$ can be shown to have a discontinuity at the center, where the profile consists of a cusped spike.

Of the five soliton parameters, namely, the amplitude $\mathcal{E}_0$, the speed V, the direction cosine α, the width L, and the frequency shift δ, only two are independent. The rest are related by the conditions

$$2\rho_s^2kv_g\mathcal{E}_0^2=\alpha^2v_g'+T=2L^2\delta$$

and $V=\alpha v_g$. Here, the quantities k, v_g, and T are characteristics associated with the whistler carrier waves.

We have demonstrated the existence of sharply peaked modulation of whistler waves. Such modulations originate from the nonlinear coupling of whistler waves with background plasma motion associated with electrostatic ion-cyclotron waves. This is in contrast to the often-discussed whistler modulation by ion-acoustic or magnetosonic waves, where the resulting pulses have smooth hyperbolic-secant-profile peaks. The physical reason for the discontinuous behavior (of the derivative) of the soliton profile may be the occurrence of a marginal balance between the dispersive and nonlinear effects, in the sense that the wave-breaking nonlinearity is barely balanced by the wave-spreading dispersion. Similar behavior exists in certain problems in hydrodynamics.[7] Physically, the spiked profile clearly cannot exist. It is expected that small collisional or thermal (Landau damping) effects will smooth out the profile at the discontinuity (of the derivative) locally, but the overall peaked (spiky) shape will remain.

Discrete, sharply peaked, whistler wave packets seem to have been observed in the ionosphere[8] and in the upstream solar wind.[9-11] In particular, observations in the foreshock region of the Earth's bow shock,[11] as well as near interplanetary shocks in the solar wind,[12] indicate the existence of electron or ion beam related whistler turbulence, which appears as spiky pulses of electric and magnetic field fluctuations. These pulses may be associated with the ion-cyclotron wave modulated whistler wave packets investigated here. The lack of quantitative data, however, prevents us from a detailed comparison of our theory with the observations. We shall nevertheless compare the observed pulse amplitude with our calculations. From the data given in Ref. 11, namely, $n_0=10\ \mathrm{cm}^{-3}$, $T_e=1$ eV, $ck/\omega=450$, $f_g=\Omega_e/2\pi=140$ Hz, and $f=\omega/2\pi=56$ Hz, we obtain $E_0^2/f\sim10^{-9}\ \mathrm{V^2/m^2Hz}$, which is rather high in comparison with the average value $10^{-11}\ \mathrm{V^2/m^2Hz}$ quoted in Ref. 11. The difference may be due to wave-dissipation mechanisms as well as the pulse chain behavior (the observed pulses are not isolated as in the theory), which were precluded in our theory. The condition that the time scale of the modulation is of the ion-cyclotron frequency (~ 0.08 Hz here) is consistent with the estimated (from the diagrams of Ref. 11) half-pulse-width of 15 sec. Unfortunately, the density fluctuations associated with the pulses do not seem to have been recorded. According to (18), the pulses are accompanied by in-phase density humps of the order $\delta n/n_0 \sim 10^{-4}$.

Finally, we point out that our investigation may find application in the problem of radio-frequency heating of plasmas, since whistler waves (but with $\omega \sim \Omega_e$) are used for electron cyclotron resonance heating. When the power is sufficiently high, modulations by low-frequency plasma motion can become important. The ion-cyclotron modulation considered here would be of particular importance if simultaneous ion-cyclotron resonance heating is used to heat the ions, since then a high level of electrostatic ion-cyclotron fluctuations would be present to enhance the modulation.

This work was supported by the Sonderforschungsbereich 162 and the AFOSR.

*Present address: Department of Physics, Auburn University, Auburn, AL 36849.

[1]R. A. Helliwell, *Whistlers and Related Ionospheric Phenomena* (Stanford Univ., Stanford, 1965).
[2]K. H. Spatschek, M. Y. Yu, and P. K. Shukla, J. Geophys. Res. 81, 1413 (1976).
[3]V. I. Karpman and H. Washimi, J. Plasma Phys. 18, 173 (1977).
[4]K. H. Spatschek, P. K. Shukla, M. Y. Yu, and V. I. Karpman, Phys. Fluids 22, 576 (1979).
[5]H. Washimi and V. I. Karpman, Zh. Eksp. Teor. Fiz. 71, 1010 (1976) [Sov. Phys. JETP 44, 528 (1976)].
[6]M. Porkolab and M. V. Goldman, Phys. Fluids 19, 872 (1976).
[7]V. I. Karpman, *Nonlinear Waves in Dispersive Media* (Pergamon, Oxford, 1975), p. 112.
[8]F. A. McNeil, J. Atmos. Terr. Phys. 37, 531 (1975).
[9]T. A. Russel, D. D. Childers, and P. J. Coleman, Jr., J. Geophys. Res. 76, 845 (1971).
[10]M. M. Hoppe, C. T. Russel, L. A. Frank, E. T. Eastman, and E. W. Greenstadt, J. Geophys. Res. 86, 4471 (1981).
[11]R. R. Anderson, G. K. Parks, T. E. Eastman, D. A. Gurnett, and L. A. Frank, J. Geophys. Res. 86, 4493 (1981).
[12]F. V. Coroniti, C. F. Kennel, F. L. Scarf, and E. J. Smith, J. Geophys. Res. 87, 6029 (1982).

The forced Toda lattice: An example of an almost integrable system

D. J. Kaup
Institute for Nonlinear Studies, Clarkson College of Technology, Potsdam, New York 13676

(Received 26 July 1983; accepted for publication 9 September 1983)

A method for solving forced integrable systems is presented. The method requires the knowledge of at least one piece of information about the solution. Once this is known, one may then construct the remainder of the solution. In this sense these systems are "almost integrable." The forced semi-infinite Toda lattice is used as an example and to illustrate the method.

PACS numbers: 03.40.Kf

I. INTRODUCTION

Although the inverse scattering transform[1] (IST) is well established as a method for solving free integrable systems, little work has been done on forced integrable systems. By "free" we mean those systems without some type of forcing term. Typical examples of free integrable systems would be the sine–Gordon equation[2]

$$\phi_{tt} - \phi_{xx} + \sin\phi = 0, \tag{1}$$

where the boundary conditions are $\phi(x\rightarrow\pm\infty,t) = 2\pi n$, or the nonlinear Schrödinger equation

$$i\psi_t = \psi_{xx} \pm 2(\psi^*\psi)\psi, \tag{2}$$

with the boundary conditions of $\psi(x\rightarrow\pm\infty,t) = \alpha$, where α is an arbitrary complex constant.[3,4] On the other hand, a "forced" system would have some forcing terms which determine much of the motion. As an example of a forced integrable system, the driven sine–Gordon chain is where Eq. (1) is valid for $x>0$, while the value of $\phi(0,t)$ is externally controlled. If one drove this system such that $\phi(0,t) = 2\pi t$, then for every one unit of time a new kink would have been injected into this sine–Gordon chain. Other examples are easily imagined.

One will note that the above-mentioned "free integrable" systems are all completely solved by the IST. And this method of solution is well known. But in general the "forced integrable" systems are not solvable, except in special cases wherein one may utilize some symmetry.[5] Otherwise most of what we know of such forced systems has been obtained by numerical methods.

If one reflects on what happens to the scattering data in a forced integrable system, one can appreciate some of the complexity of such systems. For example, in the above-mentioned driven sine–Gordon chain, the scattering data must vary as some complicated function of time, simply because in every new unit of time, an additional kink must appear, which means that a new pole in the reflection coefficient has to move across the real axis up into the upper half of the complex ζ-plane (ζ is the eigenvalue of the scattering problem). On the other hand, the time dependence for free integrable systems is quite simple. The bound-state eigenvalues are fixed in time as is also the magnitude of the reflection coefficient. Another feature of these forced integrable systems is that the Lax pair relation[6]

$$L_t = [M,L], \tag{3}$$

which for the free system is satisfied everywhere is now satisfied "almost everywhere" instead of "everywhere". Equation (3) is violated at those points where the system is being forced. It is this Lax relation which guaranteed the integrability of the free system in the first place. So if for the forced system Eq. (3) is now satisfied only almost everywhere, could we then not expect such systems to be something like "almost integrable"? Indeed, such is the case. As I shall demonstrate, given the forcing terms and only a few additional pieces of information about the system, the system then becomes completely integrable. This additional information is not independent of the forcing terms and is quite dependent on them. So there is a consistency problem. But once this additional information is obtained or known, then the remainder of the system does become completely integrable.

The remainder of the paper will be devoted to using the forced Toda lattice as an example of an almost integrable system and to illustrate these above ideas. By "forced Toda lattice" I mean the semi-infinite Toda lattice[7]

$$\dot{Q}_n = P_n, \tag{4a}$$

$$\dot{P}_n = -\exp(Q_n - Q_{n+1}) + \exp(Q_{n-1} - Q_n), \quad (n>1), \tag{4b}$$

and where Q_0 (and $P_0 = \dot{Q}_0$) are externally controlled. In other words, $Q_0(t)$ determines how the zeroth lattice particle will move and then the motion of all other particles to the right of this particle is determined by Eq. (4). This system was suggested to me by Professor Knopoff,[8] who along with T. G. Hill[9] had observed a fascinatingly regular envelope structure developing out of an apparently chaotic system. (See their Fig. 2.) An example of the same is shown in my Fig. 1, but at a different time. What one should note is the regular envelope structure to the left, whereas as one moves to the right the structure becomes more and more random and chaotic. To say the least, this is a very curious and strange behavior, and one would like to be able to understand what is happening here. In this case, the forcing of the zeroth particle is a very simple uniform forward motion $Q_0(t) = -2b_1t$, where b_1 is some negative constant. Thus the zeroth particle is being rammed into the other particles, creating a shock wave. The strange behavior is the subsequent creation of a regular envelope from out of this chaotic shock wave.

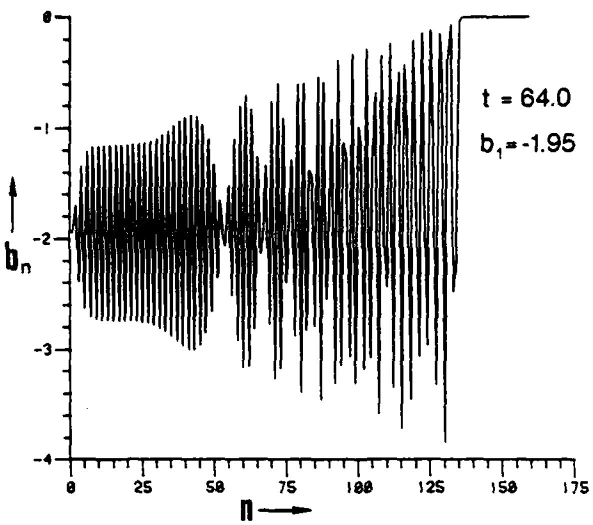

FIG. 1. Plot of b_n vs t in the forced Toda lattice for $b_1 = -1.95$ at $t = 64.0$ where $-2b_{n+1}$ is the velocity of the nth particle. Note the regular envelope structure to the right.

The study of shock waves in one-dimensional lattices is not new. An earlier analysis by Holian and Straub[10] centered on the relaxation toward thermodynamic equilibrium in the wake of shocks. Included in their numerical analysis was the Toda lattice. These numerical results for the Toda lattice have recently been intensively analyzed[11] by using local IST techniques. (By "local" IST techniques it is meant that one takes a small section of the system and analyzes it with the IST, determining what solitons are present inside this section, etc. Of course the section must be sufficiently wide so that an analysis does make sense.) This is in contrast to what I shall do here which would best be described as a "global" analysis. Thus my analysis is a compliment to theirs, and many of our results are of course the same. Mainly we differ in emphasis. Holian, Flaschka, and McLaughlin[11] sought to explain the molecular-dynamics experiments. I am seeking a more general method for determining the time evolution of the scattering data when an integrable system is being forced. Only the model and the specific results are the same. The techniques developed by each of us are different.

Next I shall briefly summarize the IST for the semi-infinite Toda lattice in Sec. II. Then in Sec. III I shall determine the time dependence of the scattering data for the forced Toda lattice. This will not be a solution of the initial-value problem since this solution will require a part of the solution before one can construct the problem. So there will be a consistency problem.

Nevertheless this solution is still useful, and in Sec. IV I shall discuss how one may use it to predict the scattering data for all time. I shall then conclude with some concluding remarks on the consistency problem.

II. THE IST FOR THE FORCED TODA LATTICE

Following Flaschka,[12] we define a_n and b_n by

$$a_{n+1} = \tfrac{1}{2}\exp[-\tfrac{1}{2}(Q_n - Q_{n-1})], \qquad (n>1), \tag{5a}$$

$$b_n = -\tfrac{1}{2}P_{n-1}; \tag{5b}$$

then from Eq. (4) it follows that

$$\dot a_n = a_n(b_n - b_{n-1}), \qquad (n>2), \tag{6a}$$

$$\dot b_n = 2(a_{n+1}^2 - a_n^2), \tag{6b}$$

where $b_1(t)$ and $Q_0(t)$ are to be specified. Equation (6) then determines a_n and b_n for $n>2$.

Consider now the eigenvalue problem[12]

$$a_{n+1}V_{n+1} + a_n V_{n-1} + (b_n - \lambda)V_n = 0 \quad (n>1), \tag{7}$$

where λ is the eigenvalue and we shall take $a_1 = \tfrac{1}{2}$ (see Ref. 13). As shown by Case[13] one may define the scattering data in the semi-infinite discrete case as follows. (I shall shift to the AKNS notation, where ψ_n are the right eigenstates and ϕ_n are the left eigenstates.) Take

$$\lambda = \tfrac{1}{2}(z + 1/z) \tag{8}$$

and assume that $a_n - \tfrac{1}{2}$ and b_n each approach zero sufficiently rapidly that the following results hold. Then the right eigenstate may be defined by

$$\psi_n(z) \to z^n \quad \text{as } n \to +\infty, \tag{9}$$

where $\psi_n z^{-n}$ is analytic inside the unit circle of the z-plane. I define

$$\bar\psi_n(z) \equiv \psi_n(1/z), \tag{10}$$

which is the second independent right eigenstate of (7).

Now define a left eigenstate by

$$\phi_n \equiv (z - 1/z)^{-1}[\bar\psi_0(z)\psi_n(z) - \psi_0(z)\bar\psi_n(z)]. \tag{11}$$

By construction,

$$\phi_0 = 0, \tag{12a}$$

$$\phi_1 = 1. \tag{12b}$$

Consider using Eqs. (7) and (12) to construct the solution ϕ_n. Clearly ϕ_n will be at most a polynomial in λ, of order $n-1$. Thus it follows that ϕ_n is analytic in λ except for a finite-order pole at $\lambda = \infty$.

Define[13]

$$S(z) = e^{2i\delta(z)} = \bar\psi_0(z)/\psi_0(z), \tag{13}$$

where δ is the phase shift. Then the scattering data consists of the values of $\delta(z)$ for z on the unit circle (the continuous spectrum) and the poles of $S(z)$ inside the unit circle (the bound-state spectrum). These poles are the zeros of $\psi_0(z)$ inside the unit circle. The bound-state part of the spectrum is specified by the value of z at the pole (z_i) and value of the normalization constant M_i^2, which is the negative of the residue of $z^{-1}S(z)$ at the pole. The constant M_i is real, whence $M_i^2>0$.

The inverse scattering equations are obtained by considering the contour integral

$$\oint_C \frac{dz}{2\pi i}\frac{\phi_n(\lambda)}{\psi_0(z)}(z - 1/z)z^{m-1}, \tag{14}$$

where C is an infinitestimal circular contour CCW around the origin. From this and upon expanding ψ_n as

$$\psi_n(z) = K_n \sum_{j=n} \kappa_{nj} z^j, \tag{15}$$

where $\kappa_{nn} = 1$, one obtains the following.[13,12] First construct

$$F_j = \frac{1}{2\pi i} \oint \frac{dz}{z} [1 - S(z)] z^j, \tag{16}$$

then for $m > n \geq 1$, one has

$$\kappa_{nm} + F_{n+m} + \sum_{j=n+1}^{\infty} \kappa_{nj} F_{j+m} = 0 \tag{17}$$

from which one may solve for $\kappa_{n,j}$. Next construct K_n from

$$(K_n)^{-2} = 1 + F_{2n} + \sum_{j=n+1}^{\infty} \kappa_{nj} F_{j+n}. \tag{18}$$

Then a_n and b_n may be recovered from

$$a_n = \tfrac{1}{2} K_n / K_{n-1}, \tag{19a}$$

$$b_n = \tfrac{1}{2} (\kappa_{n,n+1} - \kappa_{n-1,n}). \tag{19b}$$

From these equations one may construct the direct and inverse scattering transform for the forced Toda lattice. Given (a_n, b_n) for $n \geq 2$, by Eqs. (7)–(13) one may map these quantities into the scattering data. And given the scattering data, from Eqs. (16)–(19) one may construct the inverse scattering transform which allows one to reconstruct the potentials (a_n, b_n) for $n \geq 2$. Clearly we may do either of these at any time. Now the question is, if (a_n, b_n) for $n \geq 2$ evolves according to Eq. (6), how will the scattering data evolve? This we shall answer next.

III. THE TIME DEPENDENCE OF THE SCATTERING DATA

In the absence of forcing and when one has an infinite lattice, Flaschka[12] found that the time evolution of the eigenstates of Eq. (7) was given by

$$\dot{V}_n = a_{n+1} V_{n+1} - a_n V_{n-1} + C V_n, \tag{20}$$

where C is an arbitrary constant. In the infinite case, the integrability condition for (7) and (20) is the infinite Toda lattice [Eq. (6) valid for all n]. But in the semi-infinite case, although we expect Eq. (20) to be valid for large n, one must carefully account for the equations near $n = 0$ since Eq. (6) is only valid for $n \geq 2$. Equation (6) just cannot be true for $n = 1$ since a_1 and b_1 are constrained. Carefully accounting for these equations near $n = 0$ shows that for the forced Toda lattice, the equivalent form of (20) is

$$\dot{V}_n = a_{n+1} V_{n+1} - a_n V_{n-1} + C V_n \quad (n \geq 2), \tag{21a}$$

$$\dot{V}_1 = (C + \lambda - b_1) V_1 - V_0, \tag{21b}$$

$$\dot{V}_0 = (4a_2^2 - 2\dot{b}_1) V_1 + V_0 (b_1 - \lambda + C). \tag{21c}$$

We comment that Eq. (21b) is simply Eq. (21a) for $n = 1$ combined with Eq. (7) for $n = 1$. Equation (21c) follows upon differentiating Eq. (7) with respect to time. One may easily verify that the integrability conditions for Eqs. (7) and (21) are now Eqs. (6).

However, one may not uniquely determine the time evolution of the scattering data from Eq. (21). Note the term a_2^2 present in Eq. (21c). From Eq. (5) we have

$$a_2^2 = \tfrac{1}{4} \exp(Q_1 - Q_0), \tag{22a}$$

$$b_1 = -2\dot{Q}_0. \tag{22b}$$

Although we do know b_1 because $Q_0(t)$ is to be specified, we do not know what a_2^2 will be because $Q_1(t)$ is an unknown.

For the present, let us assume that we do know what a_2^2 is, and continue. To determine the time dependence of the scattering data, $S(z)$, per Eq. (13) we require the time dependence of $\psi_0(z)$. From Eqs. (9) and (21) for n large, I determine that for the eigenstate $\psi_n(z)$, the constant C is

$$C = -\tfrac{1}{2}(z - 1/z). \tag{23}$$

Define the function $\chi(z,t)$ by

$$\psi_1 = \chi e^{-Ct}; \tag{24a}$$

then by (21b),

$$\psi_0 = e^{Ct} [(\lambda - b_1)\chi - \dot{\chi}] \tag{24b}$$

and (21a) gives

$$\ddot{\chi} + \Omega^2(z,t)\chi = 0, \tag{25}$$

where

$$\Omega^2 = 4a_2^2 - \dot{b}_1 - (b_1 - \lambda)^2. \tag{26}$$

Given $\Omega^2(z,t)$ and the initial values of $\chi(z,0)$ and $\dot{\chi}(z,0)$, one may construct the solution for $\chi(z,t)$, and thereby the solution for $\psi_0(z,t)$. From Eq. (13) one may now construct the scattering function $S(z,t)$. However, the value of $4a_2^2(t)$ is required before any of this may be performed. If $4a_2^2(t)$ was known then the remainder of the solution would follow. In this sense, these forced integrable systems are "almost integrable." Some piece of the solution must be provided before the remainder of the solution will follow.

However, if one knows something nontrivial about the properties of $4a_2^2(t)$, then something nontrivial can be said about the scattering data, and thereby something nontrivial about the remainder of the solution. It is in this manner that I shall seek to glean information about this forced system.

IV. THE MOLECULAR-DYNAMICS CASE

Let us now specialize to the molecular dynamics case where one takes

$$Q_0(t) = \begin{cases} 0 & \text{if } t < 0, \\ -2b_1 t & \text{if } t > 0, \end{cases} \tag{27}$$

with b_1 as a constant, $-2b_1$ being the velocity of the zeroth particle. For this case the behavior of $4a_2^2$ is quite simple[11] and has two characteristic forms. These are shown in Fig. 2 and Fig. 3. In Fig. 2, I show the characteristic form of $4a_2^2$ for small velocities; in this example $b_1 = -\tfrac{1}{2}$. The main features to note are the initial rise, followed by a decaying ringing, which soon decays to a constant value of approximately 2.25. The value of $b_1 = -1$ is a critical value,[11] and for magnitudes of b_1 larger than this critical value the characteristic form of $4a_2^2$ changes, as one can see in Fig. 3. Here where $b_1 = -2.0$, we see that the ringing does not decay. Instead $4a_2^2$ seems to asymptotically approach an oscillation with an amplitude about 1.0 and with an average value of about 9.0.

In either case, the dominant feature of $4a_2^2$ is that it shifts from 1.0 at $t = 0$ up to some larger asymptotic value, 2.25 for $b_1 = -0.5$ and 9.0 for $b_1 = -2.0$. So as a first approximation one could replace $4a_2^2$ in Eq. (26) by its asymptotic average value and then proceed to solve for χ from Eq. (25). Of course this will not generate the exact solution for the scattering data. But one could expect that it

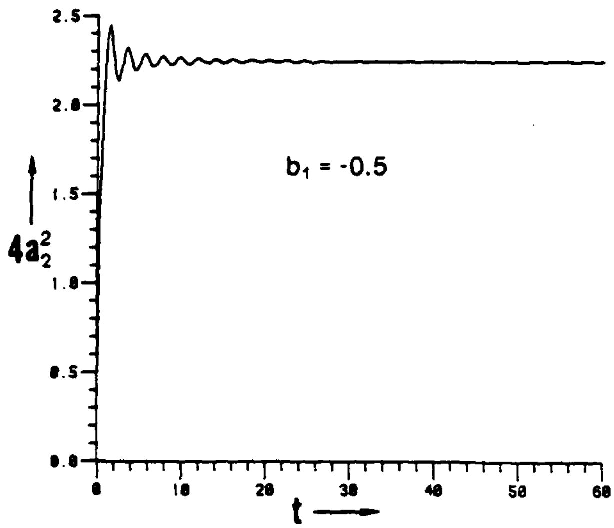

FIG. 2. A plot of $4a_2^2$ vs t when $b_1 = -0.5$ showing the rapid decay of the initial ringing.

would contain the main features of the solution. This is indeed so. We have already determined that this procedure works quite well for predicting the soliton birth rate.[14]

As a final point, I wish to point out that there may be a solution to the consistency problem such that given $b_1(t)$, one may be able to directly determine $4a_2^2$. Let me illustrate this in the molecular-dynamics case, Eq. (27). First, I determine the initial conditions on χ and $\dot{\chi}$. At $t = 0$, we have

$$a_n = \tfrac{1}{2}, \quad b_n = 0 \quad (n \geq 2), \tag{28a}$$

$$a_1 = \tfrac{1}{2}, \tag{28b}$$

while b_1 is some nonzero value. Then solving (7) for ψ_n gives

$$\psi_n = z^n \quad (n \geq 1), \tag{29a}$$

$$\psi_0 = 1 - 2b_1 z. \tag{29b}$$

So by Eq. (24) we have

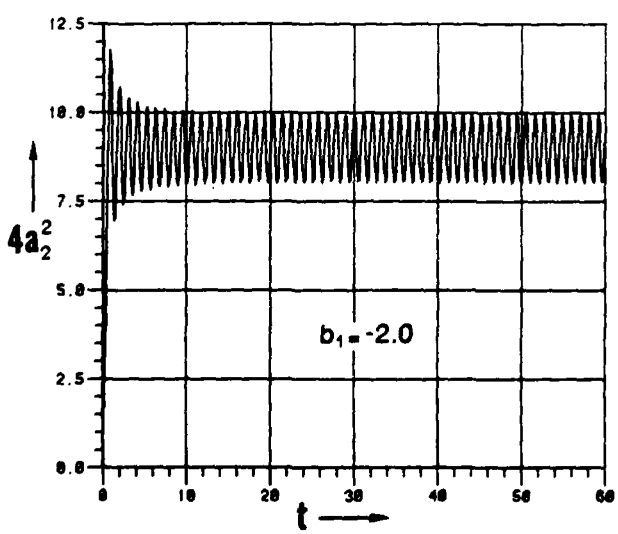

FIG. 3. A plot of $4a_2^2$ vs t when $b_1 = -2.0$ showing the asymptotic oscillations.

$$\chi(t=0) = z, \tag{30a}$$

$$\dot{\chi}(t=0) = \tfrac{1}{2}(z^2 - 1) + z b_1. \tag{30b}$$

Since b_1 is a constant, then Eq. (25) may easily be turned into the integral equation

$$\begin{aligned} 2(\lambda - b_1)\chi(t) &= z^2 \exp[(\lambda - b_1)t] + (1 - 2b_1 z)\exp[-(\lambda - b_1)t] \\ &\quad + 2\int_0^t dt'\,\chi(t')4a_2^2(t')\sinh[(\lambda - b_1)(t' - t)], \end{aligned} \tag{31}$$

where $4a_2^2$ only appears in the kernel.

Now consider the analytical properties of this solution as $|z| \to 0$. In general we would expect essential singularities at $z = 0$ due to the presence of terms like $e^{\pm\lambda t}$. But now consider (24a). We have

$$(1/z)\psi_1 = (1/z)\chi e^{Ct}, \tag{32}$$

where $(1/z)\psi_1$ is known to be analytic inside the unit circle.[13] For arbitrary values of $4a_2^2$ in (31), such will not be so on the right-hand side. One may easily verify this by using a Taylor series expansion about $t = 0$. One would also note that (32) would have the correct analytical properties only if $4a_2^2$ satisfies the equations of motion, Eqs. (6), for the proper value of b_1. (I have only checked this out to second order, but from its form, it seems reasonable that it will be true to all orders.)

This leads us to conjecture that by demanding $z^{-1}\chi e^{Ct}$ to be analytic inside the unit circle, the correct solution for $4a_2^2(t)$ may be determined and obtained without having to solve the equations of motion. Given $b_1(t)$, Eqs. (25) and (26) show that $4a_2^2(t)$ is a potential for χ, while χ satisfies a Schrödinger-like equation on the semi-infinite interval $t > 0$. Clearly, $4a_2^2$ could be mapped into the scattering data for the problem given by Eq. (25). But whether or not the required analytical properties of χ in Eq. (32) are sufficient to obtain this scattering data remains to be seen.

ACKNOWLEDGMENTS

The author gratefully acknowledges the assistance of Mr. Dan Neuberger in performing the numerical calculations and preparing the figures. He also wishes to thank Professor Knopoff and Professor Busse for their kind hospitality during the author's stay at the Institute of Geophysics and Planetary Physics, UCLA. This research has been supported in part by the Institute of Geophysics and Planetary Physics (UCLA) and the Air Force Office of Scientific Research, Air Force Systems Command, USAF, under Grant or Cooperative Agreement Number AFOSR-82-0154. This material is based upon work supported by the National Science Foundation under Grant No. MCS-8202117. Any opinions, findings, conclusions or recommendations expressed in this publication are those of the author and do not necessarily reflect the views of the National Science Foundation.

[1]M. Ablowitz, D. Kaup, A. Newell, and H. Segur, Stud. Appl. Math. 53, 249 (1974).
[2]M. Ablowitz, D. Kaup, A. Newell, and H. Segur, Phys. Rev. Lett. 30, 1262 (1973).

[3]V. E. Zakharov and A. B. Shabat, Zh. Eksp. Teor. Fiz. **61**, 118 (1971) [Sov. Phys. JETP **34**, 62 (1972)].
[4]V. E. Zakharov and A. B. Shabat, Zh. Eksp. Teor. Fiz. **64**, 1627 (1973) [Sov. Phys. JETP **37**, 823 (1973)].
[5]M. J. Ablowitz and H. Segur, J. Math. Phys. **16**, 1054 (1975).
[6]P. Lax, *Comm. Pure Appl. Math.* **21**, 467 (1968).
[7]M. Toda, Prog. Theor. Phys. Suppl. **45**, 174 (1970).
[8]L. Knopoff (private communication).
[9]T. G. Hill and L. J. Knopoff, Geophys. Res. Pap. **85**, 7025 (1980).
[10]B. L. Holian and G. K. Straub, Phys. Rev. B **18**, 1593 (1978).
[11]B. L. Holian, H. Flaschka, and D. W. McLaughlin, Phys. Rev. A **24**, 2595 (1981).
[12]H. Flaschka, Prog. Theor. Phys. **51**, 703 (1974).
[13]K. M. Case, J. Math. Phys. **14**, 916 (1973).
[14]D. J. Kaup and D. H. Neuberger, J. Math. Phys. **25**, 282 (1984).

The soliton birth rate in the forced Toda lattice

D. J. Kaup and D. H. Neuberger
Institute for Nonlinear Studies, Clarkson College of Technology, Potsdam, New York 13676

(Received 26 July 1983; accepted for publication 9 September 1983)

The soliton birth rate in the semi-infinite Toda lattice is studied. The lattice is forced by driving the zeroth particle with a constant velocity into the remainder of the lattice. An approximate solution for the soliton birth rate is derived and it is shown to compare quite favorably with the actual birth rate.

PACS numbers: 03.40.Kf

In a recent paper[1] one of the authors (DJK) discussed and demonstrated how one could solve "almost integrable" systems, one example of which is the forced Toda lattice. This is the semi-infinite Toda lattice[2] where the equation of motion is

$$\dot{Q}_n = \exp(Q_n - Q_{n-1}) - \exp(Q_{n+1} - Q_n) \tag{1}$$

for $n \geq 1$. The position of the zeroth particle $Q_0(t)$ is assumed to be driven by some external agent. And the motion of this particle then drives all other particles through Eq. (1). A simple example is a case from molecular dynamics[3] where one starts with a static lattice; then at $t = 0$ one forces the zeroth particle to ram into the remainder of the lattice by imposing upon it a uniform forward velocity. Thus $Q_0 = v_0 t$, where v_0 is a constant.

As this zeroth particle rams into the remainder of the lattice, a shock wave is created, the front part of which consists of a collection of solitons, all with approximately the same velocity. Parts of this shock wave have been analyzed[3] using "local IST" techniques to verify that solitons are present with approximately the same velocities.

With the recently developed method for handling almost integrable systems,[1] it now becomes possible to accurately predict what the soliton structure and spectrum of this shock wave is. The purpose of this paper is to predict this spectrum and to compare the predicted soliton spectrum with the actual observed spectrum. As we shall see, the agreement between the predictions and the numerical results is quite good indeed.

Next we shall summarize those equations and results from Ref. 1 which are applicable to the motion of the soliton spectrum. The solution of these equations requires one to know beforehand what will be the separation between the first two particles as a function of time. We approximate this in a reasonable manner and obtain thereby an approximate solution for the motion of the bound-state (soliton) spectrum. We next numerically compute the lattice motion from Eq. (1), determine what the actual spectrum is at various times, and then compare results.

According to Kaup,[1] the inverse scattering transform (IST) for the forced Toda lattice requires the solution of the eigenvalue problem

$$a_{n+1}\,\psi_{n+1} + a_n\,\psi_{n-1} + (b_n - \lambda)\,\psi_n = 0, \tag{2}$$

where

$$\lambda = \tfrac{1}{2}(z + 1/z), \tag{3}$$

and ψ_n is the eigensolution where

$$\psi_n \to z^n \quad \text{as} \quad n \to +\infty. \tag{4}$$

The quantities a_n and b_n in Eq. (2) are related to Q_n by

$$a_{n+1} = \tfrac{1}{2}\exp[-\tfrac{1}{2}(Q_n - Q_{n-1})], \tag{5a}$$

$$b_n = -\tfrac{1}{2}\dot{Q}_{n-1}, \tag{5b}$$

and thus as $n \to +\infty$,

$$a_n \to \tfrac{1}{2}, \tag{6a}$$

$$b_n \to 0. \tag{6b}$$

Note that b_1 is just the negative of one half of the velocity of the driven zeroth particle. Also a_1 cannot be defined by (5a) since the $n = -1$ particle does not exist. Instead we may define it to be $\tfrac{1}{2}$, as was shown by Case.[4] The bound-state eigenvalues are those values of z where $\psi_0(z)$ is zero.[4,5] These only occur when z is real and is between -1 and $+1$.

As shown by Kaup,[1] if one defines the function χ by

$$\chi = \psi_1 e^{-Ct}, \tag{7}$$

it then follows that

$$\dot{\chi} = (\lambda - b_1)\,\chi - \psi_0 e^{-Ct}, \tag{8}$$

and that χ will satisfy

$$\ddot{\chi} + \Omega^2\chi = 0, \tag{9}$$

where

$$\Omega^2(z,t) = 4a_2^2(t) - (b_1 - \lambda)^2 - \dot{b}_1 \tag{10}$$

and

$$C = -\tfrac{1}{2}(z - 1/z). \tag{11}$$

Thus if one possessed the function $\chi(z,t)$, from (8) one could construct $\psi_0(z,t)$ thereby obtaining the soliton spectrum (the zeros of ψ_0) as a function of time. However, before we may construct the solution for χ, we must know $4a_2^2$, which by (5a) is

$$4a_2^2 = \exp(Q_0 - Q_1). \tag{12}$$

Although Q_0 is given, Q_1 is not and requires the solution of the problem which we are trying to solve. For the moment we shall simply assume that $4a_2^2$ is known, and continue.

Assuming $4a_2^2(t)$ to be known, then we may solve Eq. (9) as follows. Take a solution of (9) to be of the form

 0022-2488/84/020282-03$02.50 © 1984 American Institute of Physics

$$\chi = Ae^{\pm i\phi}; \tag{13}$$

then Eq. (9) gives

$$A = \mathrm{const}/(\dot\phi)^{1/2}, \tag{14}$$

$$\dot\phi^2 = \Omega^2 + \mu^2 + \dot\mu, \tag{15}$$

where

$$\mu = \dot A/A. \tag{16}$$

The initial values for χ and $\dot\chi$ follow from the initial values for a_n and b_n as follows. Consider the moment just after $t = 0$ where b_1 has reached its nonzero uniform value. Here

$$a_n = \tfrac{1}{2} \quad (n > 1), \tag{17a}$$

$$b_n = 0 \quad (n \geqslant 2). \tag{17b}$$

We may now solve (2) for the initial value of ψ_n. We find

$$\psi_n(t=0) = z^n \quad (n > 1), \tag{18a}$$

$$\psi_0(t=0) = 1 - 2b_1 z, \tag{18b}$$

which by (7) and (8) give the initial values

$$\chi(t=0) = z, \tag{19a}$$

$$\dot\chi(t=0) = \lambda z - 1 + b_1 z. \tag{19b}$$

Matching the two possible solutions in (13) to these initial conditions, we determine the correct solution of χ to be

$$\chi = \frac{A}{A_0}\left[z\cos\phi + \frac{\dot\chi_0 - \mu_0 z}{\dot\phi_0}\sin\phi\right], \tag{20}$$

where the subscripts "0" refer to initial values and we have taken

$$\phi_0 = 0. \tag{21}$$

So far no approximations have been made. From (8), the zeros of ψ_0 will be where

$$\tan\phi = \frac{\dot\phi_0(\lambda - b_1 - \mu) + \dot\phi(1/z - \lambda - b_1 + \mu_0)}{(\lambda - b_1 - \mu)(1/z - \lambda - b_1 + \mu_0) - \dot\phi_0\dot\phi}. \tag{22}$$

Define

$$\Delta_0 = \arctan[\dot\phi_0/(1/z - \lambda - b_1 + \mu_0)] \tag{23}$$

with which Eq. (22) can be reduced to

$$\phi = \Delta_0 + \arctan[\dot\phi/(\lambda - b_1 - \mu)]. \tag{24}$$

Now, let us approximate in the spirit of the WKB method to determine $\dot\phi$ and $\dot\phi_0$. From (1), (5), (10), (14), and (16) one has that the initial value of μ is

$$\mu_0 = b_1/2\dot\phi_0^2. \tag{25}$$

Provided $\dot\phi_0$ was not close to zero, the solution of (15) would be $\dot\phi = \pm\Omega$. However, if Ω^2 would be close to zero we would have to account for the terms $\mu^2 + \dot\mu$. We do this by evaluating them for $\dot\phi_0$ small. Otherwise they would have no significant effect and could be ignored. For small $\dot\phi_0$, we have

$$\dot\mu_0 \simeq b_1^2/\dot\phi_0^4 = 4\mu_0^2 \tag{26}$$

so we approximate Eq. (15) initially by

$$\dot\phi_0^2 = 1 - (\lambda - b_1)^2 + \tfrac{1}{4}b_1^2/\dot\phi_0^4, \tag{27}$$

which is a cubic equation for $\dot\phi_0^2$. It has only one positive real root when λ and b_1 are real.

For the later times, we shall simply ignore the effects of

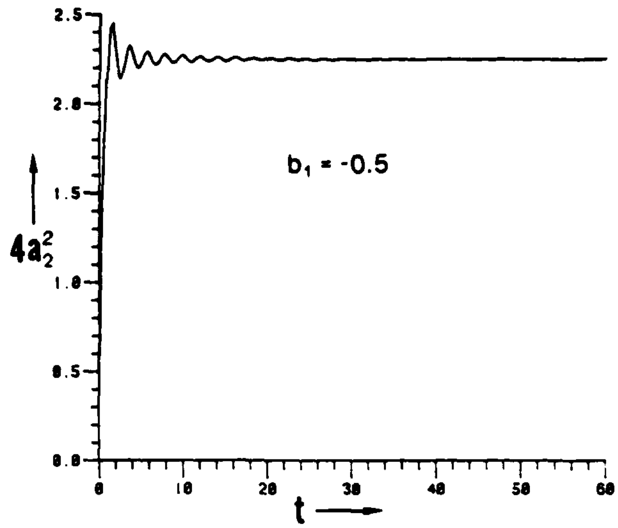

FIG. 1. A plot of $4a_2^2$ vs t when $b_1 = -0.5$ showing the rapid decay of the initial ringing.

μ and $\dot\mu$. Thus we take them to be zero in (15) and (24). It only remains to specify the values of $4a_2^2(t)$. To see how best to do this consider $4a_2^2$ vs t as shown in Fig. 1, which is when $b_1 = -0.5$, and Fig. 2 which is when $b_1 = -2.0$. What we observe there is that $4a_2^2$ rapidly shifts from its value of 1.0 at $t = 0$ to a larger average value. Clearly the most dominant feature is this definite shift in the average value. So we shall approximate the value of $4a_2^2$ required in the calculation of $\dot\phi$, Eq. (15), by its average value. Thus

$$\dot\phi^2 \simeq \langle 4a_2^2\rangle - (b_1 - \lambda)^2. \tag{28}$$

From Figs. 1 and 2, we have

$$b_1 = -0.5, \quad \langle 4a_2^2\rangle \simeq 2.25, \tag{29a}$$

$$b_1 = -2.0, \quad \langle 4a_2^2\rangle \simeq 9.0, \tag{29b}$$

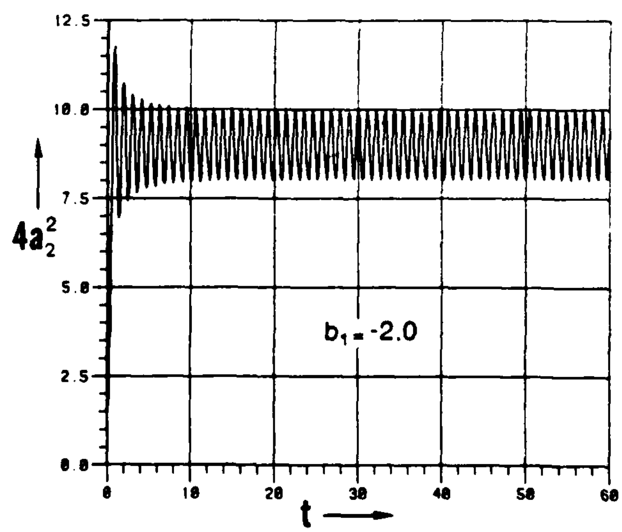

FIG. 2. A plot of $4a_2^2$ vs t when $b_1 = -2.0$ showing the asymptotic oscillations.

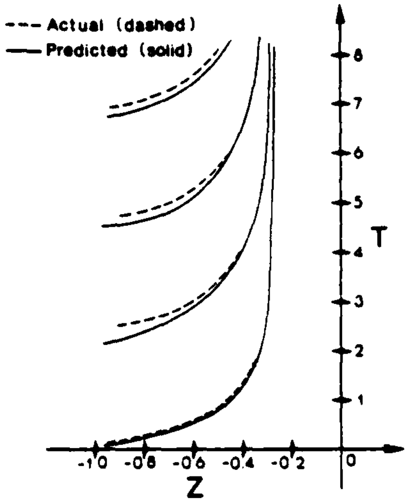

FIG. 3. The soliton birth rate when $b_1 = -0.5$ as predicted by Eq. (31) (solid line) and as actually is (dashed line).

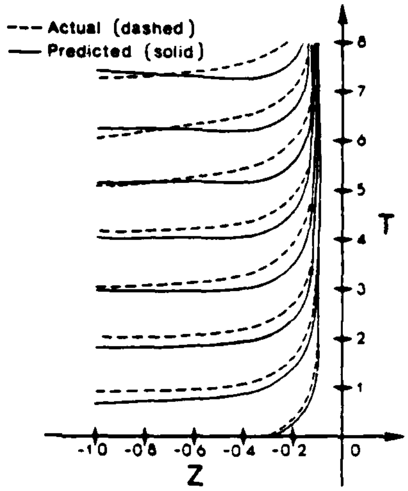

FIG. 4. The soliton birth rate when $b_1 = -2.0$ as predicted by Eq. (31) (solid line) and as actually is (dashed line).

which are the only values that we shall consider here.

Now

$$\phi = \dot{\phi} t, \tag{30}$$

and Eq. (24) gives

$$t = (\dot{\phi})^{-1}[\Delta_0 + \arctan(\dot{\phi}/(\lambda - b_1))]. \tag{31}$$

This equation gives all possible times associated with a given possible value for a bound-state eigenvalue.

A plot of these t values vs z is shown by the solid lines in Fig. 3 for $b_1 = -0.5$ and in Fig. 4 for $b_1 = -2.0$. In Fig. 3, these curves are easily interpreted as being the motion of the eigenvalues of individual solitons. The first soliton is created at $t \sim 0.1$ with an eigenvalue of just above $z = -1$. (A soliton with $z = -1$ would have a zero velocity, zero amplitude, and an infinite width. When z is just greater than -1, then these values become finite and nonzero.) This eigenvalue moves rapidly toward the limiting value of -0.29 at which all bound-state eigenvalues eventually tend to collect, as seen in Fig. 3. The motion in Fig. 4 is quite similar, except that the solitons are created at a faster rate, and the first soliton already exists at $t = 0$. The limiting value is now -0.10, which means faster and narrower solitons as one would expect.

To see how good these predictions are, let us compare this with the actual soliton spectrum. To determine this, we shall numerically integrate Eq. (1) up to some time t. At this time, we shall calculate the a_n's and the b_n's as given by Eq. (5), then solve Eq. (2) numerically for $\psi_0(z)$, plotting $\psi_0(z)$ vs z from $z = -1$ to $z = +1$. One may then easily pick out the zeros of $\psi_0(z)$ which are the bound-state eigenvalues.

The result of this are the dashed lines in Figs. 3 and 4. As seen in Fig. 3, the agreement is quite good, the only difference being slight phase shift in the initial birth times. Otherwise the eigenvalue motion is quite accurately predicted by Eq. (24). Figure 4 does not show as good an agreement, although the general shape and motion still quite accurately reflect the actual curves. This discrepancy may arise in part from ignoring the oscillations in $4a_2^2$ (see Fig. 2) which do not seem to be decaying away. They do rapidly decay away in Fig. 1, and for that value of b_1, the results shown in Fig. 3 gave excellent results.

In conclusion we have demonstrated that one can solve for the soliton spectrum, and its subsequent motion, when an integrable system is driven by forcing terms. The method does require having some particular information about the solution, so it is not a method for solving the initial-value problem. However, the information required for finding the soliton spectrum need not be detailed, and we found average values to be adequate to reproduce at least the gross features of the curves.

ACKNOWLEDGMENTS

This research sponsored by the Air Force Office of Scientific Research, Air Force Systems Command, USAF, under Grant or Cooperative Agreement Number AFOSR-82-0154. This material is based upon work supported by the National Science Foundation under Grant No. MCS-8202117. Any opinions, findings, conclusions or recommendations expressed in this publication are those of the author(s) and do not necessarily reflect the views of the National Science Foundation.

[1]D. J. Kaup, J. Math. Phys. 25, 277 (1984).
[2]M. Toda, Prog. Theor. Phys. Suppl. 45, 174 (1970).
[3]B. L. Holian, H. Flaschka, and D. W. McLaughlin, Phys. Rev. A 24, 2595 (1981).
[4]K. M. Case, J. Math. Phys. 14, 916 (1973).
[5]H. Flaschka, Prog. Theor. Phys. 51, 703 (1974).

Whistler scattering from density fluctuations in magnetized plasmas

S. N. Antani[a] and D. J. Kaup
Clarkson University, Potsdam, New York 13676

(Received 9 September 1983; accepted 6 January 1984)

Scattering of a coherent whistler from random density fluctuations is treated by a perturbation procedure. The attenuation length is calculated for scattering by a drift-wave type fluctuation model and is simply expressed as a function of the propagation angle in the limit where the whistler wavelength is long compared to a correlation length. For typical tokamak and space plasmas, this scattering becomes most important at larger angles.

I. INTRODUCTION

Wave-scattering from random fluctuations in a plasma has been a subject of extensive investigation since fluctuations of various sorts such as in the density, temperature, magnetic field, etc., are always present in a plasma. For instance, electrons in the upper atmosphere are distributed in an irregular fashion.[1] Recently density fluctuations have also been detected in a tokamak type plasma.[2,3] Thus it becomes essential to investigate and understand the influence of random fluctuations on wave propagation.

An early attempt to consider the effect of ionospheric irregularities on wave propagation was due to Budden.[4] He assumed a Gaussian model for the irregularities and suggested that the relatively few ground observations of whistlers could be explained in terms of the scattering from small irregularities having a finite elongation along the geomagnetic field. Radio wave scattering from ionospheric irregularities was considered by Simonich and Ye.[5] They considered a "bistatic" problem in which a radio wave is sent out into the upper atmosphere by a transmitter and the scattered signal is received back on earth. They could then regard the region of scattering as small compared to the distance traveled by the radio wave. Thus they used the single scattering or the first Born approximation to calculate the scattered power and the scattering cross section as a function of the random inhomogeneity of the medium. Ott[6] considered the scattering of a lower-hybrid wave from random density fluctuations using a wave kinetic formalism. Using the same formalism, Hui *et al.*[7] reported a numerical calculation of the ray trajectory modification of the electron-cyclotron wave due to the density fluctuations.

In this work we shall consider the scattering of a coherent whistler wave from random density fluctuations in a magnetized plasma. We are principally motivated by the following considerations: (i) Whistlers are known to travel long distances in the upper atmosphere being guided by the field aligned columns of ionization.[8] Since the electron distribution in the upper atmosphere is known to be irregular,[1] whistler propagation in the presence of these irregularities would be an important study. (ii) In the supplementary radio frequency heating scheme in the lower-hybrid range of frequencies, it has been suggested that the use of the "fast" or whistler wave may have some advantages over the usually considered "slow" or lower-hybrid wave.[9,10] Since the density fluctuations also occur in tokamaks,[2,3] it is then essential to consider whistler propagation in the presence of fluctuations.

We shall follow a perturbation procedure due to Keller[11] to study the whistler scattering problem. An important advantage of this method is that one can evaluate the final results for both the long as well as the short wavelength limits. Treating the fluctuations to be weak on a homogeneous background plasma, first a modified dispersion relation in the presence of fluctuations will be derived. It will be seen that the fluctuations cause the wave refractive index to be complex, with the real part representing the change in the phase velocity of the wave and an imaginary part signifying attenuation of the primary wave due to scattering from fluctuations.

Keller's method was employed by Liu[12] to study the scattering of the ordinary and extraordinary waves in a magnetized plasma. Satya and Schmidt[13] applied it to the problems of laser and Alfven-wave scattering from fluctuations in a plasma.

In the next section we shall describe the formalism used to derive the general dispersion relation in the presence of fluctuations. Specialization to the case of a whistler will be the topic of Sec. III. Here we shall define an attenuation length for a whistler wave, which can be interpreted as a distance over which the coherent form of the wave energy is lost. This wave energy then reappears as an incoherent whistler energy. Thus another way of describing what is occurring is to say that the coherence of the beam is gradually being eaten away by the fluctuations. Next, in Sec. IV, we shall evaluate the attenuation length of the coherence for the typical parameters of tokamak and space plasmas. Finally, in Sec. V, we summarize the main conclusions and also make some pertinent remarks.

II. FORMULATION AND BASIC EQUATIONS

First we shall state the basic assumptions involved: (i) Consider a cold, collisionless and homogeneous plasma immersed in a steady magnetic field directed along the z axis. (ii) In order that the perturbation expansion be applicable, we shall assume that the fluctuations are small over a uniform background plasma. (iii) We shall treat the fluctuations as quasistatic so that the frequency characterizing the fluctuations may be taken to be much smaller than that of the whistler wave. (iv) The fluctuation spectrum is chosen to be

[a] Present address: UCLA Plasma Physics Group, Los Angeles, CA 90024.

 0031-9171/84/051169-07$01.90 © 1984 American Institute of Physics

of a Gaussian shape for analytic simplicity. This choice of a Gaussian shape is further motivated by the fact that the observed spectrum can be closely approximated by a Gaussian.[2,3] (v) In keeping with the observations,[2,3] we shall also assume that the fluctuation spectrum is isotropic in a plane perpendicular to the direction of the external magnetic field (i.e., the z axis). Further, since the fluctuations are mostly field-aligned, i.e., the density distribution is stratified along the ambient magnetic field, we shall ignore their effect on the z component of the wave refractive index (n_z). We shall also regard the spectrum as a function of x and y only and take the correlation length L_T to be the same in these directions. (vi) We shall consider the whistler frequency ω_0 to be in the lower-hybrid range, i.e., $\Omega_i \ll \omega_0 \ll \Omega_e$ with Ω_α denoting the cyclotron frequency of species α. This is the frequency range of interest in the rf heating of thermonuclear plasmas.[9] Whistlers in this frequency range also occur in space plasmas.[14]

Assuming time harmonic solutions, the Maxwell equations can be written in the form,

$$\nabla\times\nabla\times\mathbf{E} = \mathsf{K}\cdot\mathbf{E}, \tag{1}$$

where the spatial variables have been normalized in units of ω_0/c and K is the cold plasma dielectric tensor given by

$$K = \begin{bmatrix} K_\perp & -iK_x & 0 \\ iK_x & K_\perp & 0 \\ 0 & 0 & K_\parallel \end{bmatrix}, \tag{2}$$

where the elements $K_\perp$, K_x, and $K_\parallel$ are defined as follows:

$$K_\perp \approx 1 - \omega_{pi}^2/\omega^2 + \omega_{pe}^2/\Omega_e^2, \tag{3a}$$

$$K_x \approx \omega_{pe}^2/\omega_0\Omega_e, \tag{3b}$$

$$K_\parallel \approx -\omega_{pe}^2/\omega_0^2. \tag{3c}$$

Here $\omega_{p\alpha}$ is the plasma frequency of species α.

If there were no fluctuations, then we know that Eq. (1) would just provide us with the usual linear description of the waves. Because of the presence of the density fluctuations, however, the density-dependent parts of the cold plasma dielectric tensor K are modified. Then one can expresses Eq. (1) in the form of a general stochastic equation (i.e., a partial differential equation with random coefficients),

$$\mathscr{L}E = 0, \tag{4}$$

where $\mathscr{L}$ is the stochastic differential operator (matrix), and E is a random wave field. It is convenient to separate out the part due to fluctuations from the general Maxwell operator $\mathscr{L}$ in the basic equation (4). This is done simply by writing the dielectric tensor elements formally as,

$$K_\perp = K_{\perp 0} + (K_{\perp 0} - 1)(\delta n/N_0), \tag{5}$$

$$K_x = K_{x0}(1 + \delta n/N_0), \tag{6}$$

$$K_\parallel = \kappa_{\parallel 0}(1 + \delta n/N_0), \tag{7}$$

where the quantity $(\delta n/N_0)$ arises due to the density fluctuations and the quantitites with zero subscript are the unperturbed parts evaluated at the ambient plasma density.

With these developments, we can split Eq. (4) as follows:

$$\mathscr{L}E = (L + V)E = L(1 + L^{-1}V)E = 0. \tag{8}$$

Here, L represents the nonrandom part of the operator, while V stands for the fluctuating part. The above equation tacitly assumes that the inverse of L exists. The justification of this assumption comes from the consideration that the fluctuations alter the wave refractive index, so that in their presence the determinant of L is nonzero. Further, the fluctuating part V can be expressed as

$$V = (\delta n/N_0)M \tag{9}$$

and M is the constant matrix,

$$M = \begin{pmatrix} -(K_{\perp 0} - 1) & iK_{x0} & 0 \\ -iK_{x0} & -(K_{\perp 0} - 1) & 0 \\ 0 & 0 & -K_{\parallel 0} \end{pmatrix}. \tag{10}$$

Basically Keller's method involves the derivation of an equation for the averaged field in the presence of fluctuations.[11] To derive such an equation, begin with Eq. (4) and write the stochastic operator $\mathscr{L}$ as follows:

$$\mathscr{L} = [\mathscr{L}^{-1}]^{-1} = \{(1 + L^{-1}V)^{-1}L^{-1}\}^{-1}. \tag{11}$$

Next, consider the binomial expansion for $(1 + L^{-1}V)^{-1}$,

$$(1 + L^{-1}V)^{-1} = \sum_{n=0}^{\infty}(-L^{-1}V)^n. \tag{12}$$

This requires that $|L^{-1}V| < 1$. Thus, one must estimate the magnitude of this last quantity to ensure that the binomial expansion as such will be applicable in a given problem. For now, it will be assumed that $|L^{-1}V|$ is sufficiently small to permit dropping of terms up to and higher than $(L^{-1}V)^3$. This will be *a posteriori* justified later in this paper.

Next, rewrite Eq. (4) using Eqs. (11) and (12) and consider the ensemble average of the resulting equation, i.e.,

$$\left\langle L\left[\sum_{m=0}^{\infty}(-1)\sum_{n=1}^{\infty}(-L^{-1}V)^n\right]^m E\right\rangle$$
$$= [L + \langle V\rangle - \langle VL^{-1}V\rangle + \langle V\rangle L^{-1}\langle V\rangle + O(L^{-1}V)^3]\langle E\rangle = 0, \tag{13}$$

where the angle brackets indicate an ensemble average. If $\langle V\rangle = 0$, and the terms of order $(L^{-1}V)^3$ and higher are ignored in the above equation, then one obtains Keller's equation,

$$L\langle E\rangle = \langle VL^{-1}V\rangle\langle E\rangle. \tag{14}$$

The inverse operator L^{-1}, or the Green's function, is defined such that,

$$LG(\mathbf{r},\mathbf{r}') = \mathsf{I}\delta(\mathbf{r} - \boldsymbol{\gamma}'), \tag{15}$$

where $G(\mathbf{r},\mathbf{r}')$ is the usual Green's function or in this case a Green's matrix. We may also write down the following Fourier representation for Green's matrix $G(\mathbf{r},\mathbf{r}')$, obtained by simply taking the Fourier transform of Eq. (15):

$$G(\mathbf{n},\mathbf{n}') = \frac{\mathsf{I}\delta(\mathbf{n} + \mathbf{n}')\tilde{L}(n)}{|L(n)|}, \tag{16}$$

where, $\tilde{L}(\mathbf{n})$ represents the transposed matrix of cofactors of L and $|L(\mathbf{n})|$ is the determinant of L. In terms of G, L^{-1} can be expressed as an integral operator,

$$L^{-1}V = \int d^3r'\, G(\mathbf{r},\mathbf{r}')V(\mathbf{r}'). \tag{17}$$

Consequently, Eq. (14) becomes

$$L\langle E\rangle = \left\langle \int d^3r'\, V(\mathbf{r})G(\mathbf{r},\mathbf{r}')V(\mathbf{r}')\langle E(\mathbf{r}')\rangle\right\rangle. \tag{18}$$

From Eq. (18) one can readily derive the dispersion relation using the standard Fourier technique.[11] The result can be expressed as follows:

$$\det\left(L(\mathbf{n}) - \frac{1}{(2\pi)^{3/2}}\int d^3n' \frac{M\tilde{L}(\mathbf{n}')M}{|L(\mathbf{n}')|}\sigma(\mathbf{n}-\mathbf{n}')\right) = 0. \tag{19}$$

In Eq. (19), we have defined a two-point correlation function $\sigma(n-n')$ such that

$$\frac{\langle \delta n(r)}{N_0}\frac{\delta n(r')\rangle}{N_0} = \sigma(\mathbf{r}-\mathbf{r}'),$$

i.e., the medium is statistically homogeneous. We could solve Eq. (19) for different forms of the correlation spectrum such as Gaussian, exponential, Lorentzian, etc. As mentioned in assumption (iv) at the beginning of this section, we shall illustrate the calculations for a Gaussian spectrum. Thus take

$$\sigma(\mathbf{n}-\mathbf{n}') = \epsilon^2\bar{l}^2 \exp[|\mathbf{n}_\perp - \mathbf{n}'_\perp|^2\bar{l}^2/2]\delta(n_z - n'_z), \tag{20}$$

where $n_\perp = k_\perp c/\omega_0$ is the perpendicular component of the propagation vector and $\bar{l} = \omega_0/L_T/c$ is the normalized correlation length. Further, $\epsilon = \langle(\delta n/n_0)^2\rangle^{1/2}$ is the measure of the strength of the fluctuations. Note that if $\epsilon = 0$, i.e., if there were no fluctuations, the solution to Eq. (19) would yield the usual dispersion relations of the characteristic modes.

III. ANALYSIS OF THE GENERAL DISPERSION EQUATION

First, we remark that Eq. (19) contains two cold plasma modes. One of these is the "slow" or lower-hybrid mode and the other one is the "fast" or the whistler mode. Our object is to focus on the latter mode. To this end, we need only to recall that the whistler mode polarization is such that $|E_z| \ll |E_x|$ or $|E_y|$, i.e., we can neglect $|E_z|$ compared with either $|E_x|$ or $|E_y|$ in the frequency range of interest.[8] Then we can approximate the 3×3 matrix L to the following 2×2 matrix

$$L \simeq \begin{pmatrix} K_{\perp 0} - n_z^2 - n_\perp^2 \sin^2\phi & -iK_{x0} + n_\perp^2 \sin\phi\cos\phi \\ iK_{x0} + n_\perp^2\sin\phi\cos\phi & K_{\perp 0} - n_z^2 - n_\perp^2\cos^2\phi \end{pmatrix}. \tag{21}$$

The corresponding matrix M is

$$M \simeq \begin{pmatrix} -(K_{\perp 0} - 1) & iK_{x0} \\ -iK_{x0} & -(K_{\perp 0} - 1) \end{pmatrix}. \tag{22}$$

We note from Eq. (21) that the whistler dispersion relation follows from the solution to $|L(n)| = 0$, i.e.,

$$n_{\perp 0}^2 \simeq K_{x0}^2/(n_z^2 - K_{\perp 0}) - (n_z^2 - K_{\perp 0})$$
$$\simeq K_{x0}^2/n_z^2 - n_z^2, \quad \text{if } n_z^2 \gg K_{\perp 0}. \tag{23}$$

To evaluate the integral in Eq. (19), we choose a coordinate system such that $\mathbf{n}_\perp = n_\perp\hat{x}$, and let ϕ be the scattering angle. Then the exponent in Eq. (20) can be written,

$$|\mathbf{n}_\perp - \mathbf{n}'_\perp| = n_\perp^2 + n_\perp'^2 - 2n_\perp n'_\perp\cos\phi. \tag{24}$$

Also, $dn' = dn'_x\, dn'_y dn'_z = n'_\perp\, dn'_\perp\, dn'_z\, d\phi$. With these preliminaries we can evaluate the $n'_\perp$-integral in Eq. (19) by noting that the integrand is singular at the roots of $|L(n')| = 0$, on the real axis. For a forward propagating incident wave, the appropriate contour passes an infinitesimal distance below the pole. Then the imaginary contribution can be simply found by using the Cauchy principal value formula. The integral over n'_z is trivial due to the delta function. Finally, for the angle integration we use the integral representation of the modified Bessel functions.[15] After evaluating the integrals for each matrix element in Eq. (19) and some algebra, we can write the expressions for the real and imaginary parts of the complex refractive index $n_\perp$ in the following compact forms:

$$\mathrm{Re}(n_\perp^2) = \left(n_{\perp 0}^2 - \frac{[(n_z^2 - K_{\perp 0})(I_{11}^2 + I_{12}^2) + 2K_{x0}I_{11}I_{12}]}{(n_z^2 - K_{\perp 0})^2}\right)\left(1 + \frac{I_{11}^2}{(n_z^2 - K_{\perp 0})^2}\right)^{-1} \tag{25}$$

$$-\mathrm{Im}(n_\perp^2) = \left(I_{22} + \frac{[2K_{x0}I_{12}(n_z^2 - K_{\perp 0}) + I_{11}(K_{x0}^2 - I_{12}^2 + I_{11}I_{22})]}{(n_z^2 - K_{\perp 0})^2}\right)\left(1 + \frac{I_{11}^2}{(n_z^2 - K_{\perp 0})^2}\right)^{-1}. \tag{26}$$

In Eqs. (25) and (26) the quantities I_{ij} arise due to the fluctuations and are defined in the following relations:

$$I_{11} = \Lambda(\alpha F_0(s) + \beta F_1(s)), \tag{27}$$

$$I_{12} = -I_{21}$$
$$= -\frac{\Lambda}{2}\frac{F_0(s)K_{x0}(n_z^2 - 1)[K_{x0}^2 + (n_z^2 - K_{\perp 0})(K_{\perp 0} - 1)]}{(n_z^2 - K_{\perp 0})^2}, \tag{28}$$

$$I_{22} = \Lambda(\alpha' F_0(s) - \beta F_1(s)), \tag{29}$$

where

$$F_0(s) = I_0(s^2)e^{-s^2},$$
$$F_1(s) = I_1(s^2)s^{-2}e^{-s^2},$$
$$\Lambda = (\pi/2)^{1/2}(\epsilon^2\bar{l}^2),$$

and I_0 and I_1 are the modified Bessel functions order zero and one, respectively. Their argument is $s^2 = n_{\perp 0}^2\bar{l}^2$, $n_{\perp 0}$ being the unperturbed perpendicular refractive index given by the linear dispersion relation (23), and $\bar{l}$ was defined just below Eq. (20). We have also defined

$$\alpha = \frac{-K_{x0}^2(n_z^2 - 1)^2}{(n_z^2 - K_{\perp 0})^2}, \tag{30}$$

$$\alpha' = \frac{-[K_{x0}^2 + (n_z^2 - K_{\perp 0})(K_{\perp 0} - 1)]^2}{(n_z^2 - K_{\perp 0})^2}, \tag{31}$$

$$\beta = \frac{-[K_{x0}^2 - (K_{\perp 0} - 1)^2][K_{x0}^2 - (n_z^2 - K_{\perp 0})^2]}{(n_z^2 - K_{\perp 0})^2}. \tag{32}$$

Naturally one may note from the relations (25) and (26) that in the absence of fluctuations, the I_{ij}'s vanish giving $\mathrm{Re}(n_\perp) = n_{\perp 0}$ and $\mathrm{Im}(n_\perp) = 0$ as expected.

Equation (25) expresses the change in the real part of the refractive index due to the fluctuations. This in turn means that the wave velocity experiences only second-order changes due to density perturbations. On the other hand, Eq. (26) says that the primary wave is being attenuated by the presence of the fluctuations as the wave energy scatters off them and is a first-order change. One can define the attenuation length as follows:

$$l_a = c/[2\omega_0 \mathrm{Im}(n_\perp)]. \tag{33}$$

This is the distance over which the coherent energy from the primary wave is lost to the fluctuating components.

Before discussing applications of the basic results of this section, namely Eqs. (25) and (26), let us consider two limiting forms of these equations. These correspond to the small and large argument limits of the modified Bessel functions.[15]

(*i*) *$s^2 \ll 1$, or the long wavelength limit*: In this case we can use the small argument expansions of the Bessel functions.[15] We thus have, $F_0(s) \simeq 1$ and $F_1(s) \simeq 1/2$. We shall find that for most applications we have in mind, the dielectric tensor element $K_{x0} \gg 1$ and that $K_{x0} \gg K_{\perp 0}$. Further, it can be shown *that $n_z^2 = K_{x0} \cos\theta_0$, where θ_0 is the propagation angle relative* to the background magnetic field. Using this fact and retaining only the dominant contributions, these arguments simplify Eqs. (25) and (26) as follows:

$$\mathrm{Re}(n_\perp^2) = n_{\perp 0}^2 + O(\Lambda^2), \tag{34}$$

$$\mathrm{Im}(n_\perp^2) = \frac{\Lambda K_{x0}^2}{2} \frac{(1 + 4\cos^2\theta_0 + \cos^4\theta_0)}{\cos^4\theta_0} + O(\Lambda^2). \tag{35}$$

(*ii*) *$s^2 \gg 1$, or the geometric optics* (*short wavelength*) *limit*: In this case, the random inhomogeneity scale length is large compared to the whistler wavelength. Thus we can use the asymptotic forms of the Bessel functions,[15]

$$I_\nu(s^2) \sim \frac{e^{s^2}}{(2\pi s^2)^{1/2}}\left[1 + O\left(\frac{1}{s^2}\right)\right],$$

where $\nu = 0,1$. Then we have

$$F_0(s) \sim \frac{1}{(2\pi s^2)^{1/2}}, \quad F_1(s^2) \sim \frac{1}{s^2}\frac{1}{(2\pi s^2)^{1/2}}.$$

In this case we find

$$I_{11} \simeq [\Lambda/(2\pi s^2)^{1/2}(\alpha + \beta/s^2)], \tag{36}$$

$$I_{12} = I_{21} = \frac{-\Lambda K_{x0}}{2(2\pi s^2)^{1/2}} \frac{(K_{x0}\cos\theta_0 - 1)}{\cos^2\theta_0}, \tag{37}$$

$$I_{22} = [\Lambda/(2\pi s^2)^{1/2}](\alpha' - \beta/s^2). \tag{38}$$

With these, Eqs. (25) and (26) become

$$\mathrm{Re}(n_\perp^2) = n_{\perp 0}^2 + O(\Lambda^2), \tag{39}$$

$$\mathrm{Im}(n_\perp^2) = [\Lambda K_{x0}^4/(2\pi s^2)^{1/2}\cos^2\theta_0] + O(\Lambda^2). \tag{40}$$

It should be kept in mind that this limit is meaningful only if s^2 is such that it satisfies the condition $|L^{-1}V| \ll 1$. More on this will be said later.

We shall now discuss the implications of these results in the next section.

TABLE I. Typical plasma parameters.

Parameters	Tokamak	Ionosphere (F layer)	Plasmasphere (4 earth radii)
Whistler frequency ω_0(rad sec^{-1})	5×10^9	5×10^4	5×10^3
Electron density N_0(cm^{-3})	2×10^{13}	10^6	10^2
Magnetic field, B_0 (Gauss)	2×10^4	4.8×10^{-1}	5×10^{-1}
Electron temp. T_e(eV)	10^3	1.5×10^{-1}	1
Ion temp. T_i(eV)	200	3×10^{-2}	1

IV. APPLICATIONS

To discuss the implications of the results of the last section, let us begin by listing the typical plasma parameters of interest in Table I. A glance at Eqs. (25) and (26) reveal that the knowledge of the dielectric tensor elements K_{x0} and $K_{\perp 0}$ is also required. The estimates of these in the frequency range of interest are given in Table II.

For the subsequent discussion it will be helpful to recall from the whistler propagation theory[8] that in the chosen frequency regime, the whistler propagation angles can have a wide range of values with the upper bound determined by the condition that the refractive index remain real. On the other hand, the group velocity (ray) direction remains within a maximum of 19.5 deg relative to the background magnetic field. In what follows we shall examine the behavior of the attenuation length as a function of the propagation angle of a whistler wave.

The next task is to have the estimates of the fluctuation level ϵ and the correlation length L_T. For this purpose we need to invoke a suitable model. We shall choose a model deduced from observations[2,3] according to which the fluctuations are caused by drift-wave type turbulence. Drift waves are the characteristic modes of an inhomogeneous plasma. The extremely low-frequency (ELF) electric field fluctuations observed near the plasmapause (boundary of the plas-

TABLE II. Estimates of dielectric tensor elements in LH range.

Element	Tokamak	Ionosphere (F layer)	Plasmasphere (4 earth radii)
K_{x0}	36	7.5×10^3	7.2×10^2
$K_{\perp 0}$	0.12	6.3	35

TABLE III. Estimates of ϵ and L_T for drift-wave model.

Parameter	Tokamak	Ionosphere (F layer)	Plasmasphere (4 earth radii)
L_n cm	10	10^7	6.4×10^7
L_T cm	7.2×10^{-2}	1.6×10^2	$2\ \times10^4$
ϵ	7.3×10^{-3}	1.6×10^{-5}	3.1×10^{-4}

masphere) region can be explained in terms of the drift instability.[16] In the equatorial F region of the ionosphere, drift waves presumably dominate for wavelengths $\lambda \lesssim 100$ m.[1]

Thus adopting this drift-wave model we can assume[2,3] the following empirical scaling:

$$L_T \sim \rho_i, \tag{41}$$

$$\epsilon \sim L_t / L_n, \tag{42}$$

where $\rho_i = v_{ti}/\Omega_i$ (v_{ti} is the ion thermal speed) is the ion gyroradius and L_n is the scale length of the regular density gradient. For the present discussion, we have $L_n \gg L_T$. Table III presents estimates of ϵ and L_T for the chosen parameters.

A. Case 1. Tokamak plasma

First we note that in order for the plasma interior to be accessible to the externally launched rf wave, the parallel-refractive index is limited to a rather narrow spectrum.[9] Typically, $1.3 < n_z < 3$. Now for the whistler wave, we have $n_Z^2 = K_{X0} \cos\theta_0$ so that the accessible n_z values correspond to the propagation angle range of 75.6–87.3 deg for the K_{x0} value appearing in Table II. Estimating the perpendicular refractive index n_{10} from the whistler dispersion relation for the allowed n_z values and taking the value for the correlation length L_T from Table III, we find that $s^2 = (n_{10}\bar{l})^2 \ll 1$. Thus, we use the appropriate limiting forms of the real and imaginary parts of the refractive index given by Eqs. (34) and (35), respectively. To the leading order, we see that the real part of the refractive index is unchanged, while the imaginary part can be used in the definition of the attenuation length [Eq. (33)] to get

$$l_a \approx \frac{1}{(2\pi)^{1/4}}\left(\frac{c}{\omega_{pe}}\right)\left(\frac{\Omega_e}{\omega_{pe}}\right)\left(\frac{1}{\epsilon\bar{l}}\right) \times\left(\frac{\cos^2\theta_0}{(1+4\cos^2\theta_0+\cos^4\theta_0)^{1/2}}\right). \tag{43}$$

Equation (43) makes the θ_0 dependence of the attenuation length explicit. Figure 1 shows the plot of the normalized attenuation length (l_a/a), a being the minor radius of the tokamak. We notice from this plot that the ratio (l_a/a) drops as a increases in the chosen range. This indicates increased scattering from the density fluctuations and the consequent loss of coherence of the primary whistler wave.

B. Case 2. Ionospheric (F-layer) plasma

Consider a typical whistler propagating in the F region of the ionosphere. Calculating n_{10} from the linear dispersion relation for different values of the propagation angles θ_0 and picking the L_T value from Table III under the ionosphere column, we again find that $s^2 \ll 1$, thus allowing the use of the

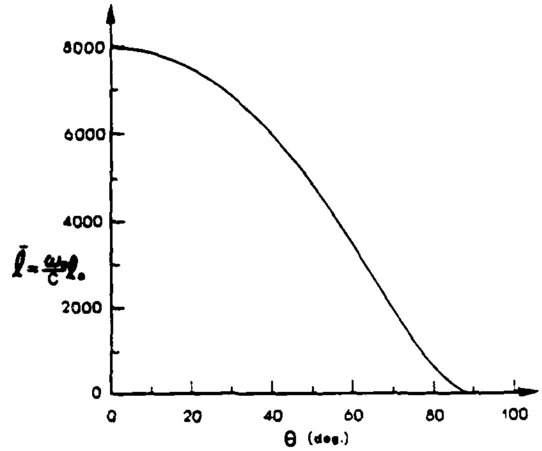

FIG. 1. Normalized attenuation length versus angle (tokamak plasma).

approximate Eq. (43). In Fig. 2 we have plotted the normalized attenuation length ($\bar{l}_a = \omega_0 l_a / c$) as a function of the propagation angle θ_0.

We notice from Fig. 2 that l_a decreases with the increase of θ_0. For the model being considered, l_a is of order 10^5 km.

C. Case 3. The plasmapause region

The drift waves presumably dominate in this region located at about 4 earth radii. Thus we can again apply the fluctuation model being considered. Using the L_T values from Table III and knowing n_{10} from the dispersion relation, we find that the long wavelength limit is again adequate. Thus making use of Eq. (43), we find that the behavior of $\bar{l}_a$ vs θ_0 is qualitatively the same as in ionosphere, but here l_a is of order 10^4 km. Comparison of this value with the correlation length and the scale length of the regular density gradient given in Table III shows that is larger than both these lengths. Within the fluctuation model being considered, we would expect then that the loss of coherence of a

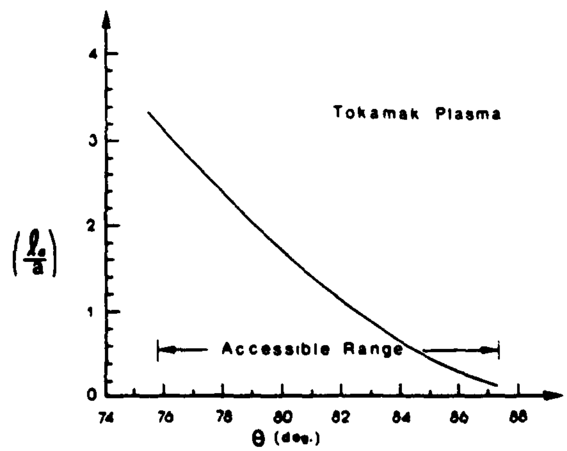

FIG. 2. Attenuation length versus angle (ionosphere).

whistler wave due to scattering from fluctuations in the plasmapause region to be insignificant.

V. CONCLUSIONS AND REMARKS

In this paper we have considered the scattering of a whistler wave from random density fluctuations in a magnetized plasma. We derived a modified dispersion relation of the wave by using Keller's method assuming the randomness to be small compared to the nonrandomness. Although we discussed only the case of a Gaussian correlation spectrum, other forms could be readily included.

The expression for the attenuation length was simplified and was examined for the scattering from short wavelength fluctuations. The results, in particular, showed that scattering becomes important as the propagation angle increases. We should remark here that the model used to estimate the correlation length and the level of fluctuations is not expected to be always valid. In particular, quite large fluctuation levels (about 30% or more) have been reported in the Alcator tokamak.[2] When the fluctuations become this strong, the perturbation method used here may of course be questioned. However, these results may still be used to develope a qualitative understanding. Nevertheless, for any detailed or rigorous analysis, there is definitely a need for some techniques designed to handle strong fluctuations.

Also, at the present time it is not clear how to predict, in a reliable manner, the fluctuation levels in the future reactor size devices. Consider, for example, a reactor size D-T plasma device with fluctuation level of 1%, minor radius $= 270$ cm, $N_0 = 10^{14}$ cm^{-3}, $B_a = 32$ kG, $n_z^2 = 10$, $T_i = 8$ keV, $\omega_0 = \sqrt{2}\omega_{lh}$, where $\omega_{lh} = \omega_{pi}(1 + \omega_{pe}^2/\Omega_e^2)^{-1/2}$ is the lower-hybrid frequency. For this case, $s^2 = 5.6$ and reading the Bessel function values from the table,[15] we find that the ratio (l_a/a) is of order 10^{-3}, indicating severe attenuation due to scattering before the wave has a chance to penetrate even one percent of the distance to the center. This essentially stems from the large size of the device. We also remark that fluctuations of other kinds, such as those in the magnetic field, also occur in tokamaks and these need to be included in a more complete theory. But these calculations do demonstrate the importance of scattering from random density fluctuations.

As one can note, the attenuation length is obtained from the modified dispersion relation of the wave in the presence of the fluctuations and it does not carry any information on the evolution of the wave field itself. To gain an insight into this question of how the field actually evolves in the presence of fluctuations, one must consider the evolution equation for the field. Start for this purpose from the equation for the averaged field given in Eq. (14) and perform the standard multiple scale analysis on this equation.[17] As a result one obtains the following linear equation:

$$i\partial_x\phi + P\partial_y^2\phi + Q\phi = 0. \qquad (44)$$

This equation assumes that the parallel refractive index of the wave is not changed due to the fluctuations. Further, the coefficient P stands for the dispersion, and is defined as

$$P = -\frac{1}{2}\frac{d^2 n_x}{dn_y^2},$$

while Q is the pure imaginary loss term due to attenuation. Equation (44) describes the linear spatial evolution of the wave field taking account of the attenuation due to scattering. This equation is reminiscent of the neutron diffusion equation in a nuclear reactor[18] where it describes the slowing down and diffusion of neutrons in a moderator with the loss term signifying the absorption. In the present discussion no diffusion occurs in the limit considered, but only pure attenuation of the primary whistler occurs as it scatters off the density fluctuations.

From what has been said thus far, we only know that some of the coherent wave energy lost due to scattering gets transformed into the incoherent form. It might be of interest to ask how does one calculate this incoherent part of the intensity. For this purpose one would have to reconsider the basic equations (4) and (14), noting that E in (4) is the total field and $\langle E \rangle$ occurring in Eq. (14) is the same as the coherent field. Then writing $E = E_i + E_c$, and taking the difference of these equations, one gets the equation for the incoherent field. It is this latter equation that one must solve to find the incoherent part of the field.[11] Note that in the model being considered the energy in the fluctuating components would remain in the wave field only. Its transfer to the particles could be predicted not from the present model but from a model that would include the appropriate wave–particle coupling. Thus within the present model, imagining the primary whistler as a radiating antenna, one could say that as the wave propagates in the presence of fluctuations, it would radiate incoherent waves at the same frequency but different harmonics of the wavenumbers. This radiated wave energy would be removed from the main whistler and would pervade the rest of the plasma in a turbulent form.

Finally, consider the question of the range of validity of Keller's method. As has been previously noted, one must estimate the magnitude of the quantity $|L^{-1}V|$ for this purpose. Now L^{-1} is some function of the wave refractive index modified by the fluctuations (i.e., if n is the effective index of refraction with $n = n^0 + n'$, where n^0 is the unperturbed value and n' is the small perturbed part introduced by the fluctuations). Then expanding L^{-1}, one finds to the leading order that L^{-1} is of order $(\mathrm{Im}\, n_\perp/n_\perp)$. Now the fluctuating part V is of order ϵ, where ϵ denotes the strength of the fluctuations. Thus one has $|L^{-1}V|$ to be of order $(\mathrm{Im}\, n_\perp/n_\perp)\epsilon$. For the whistler case, from the matrix (21) one can show that $|L^{-1}V|$ goes like $(s\epsilon^2)K_{x0}^2$, so that the condition $|L^{-1}V| < 1$ becomes

$$s \ll 1/\epsilon^2 K_{x0}^2. \qquad (45)$$

This sets a limit to the value of the parameter s up to which the binomial expansion (12) could be safely applied. Taking the typical K_{x0} values listed in Table II and the values of the fluctuation level ϵ as given in Table III, we find that Keller's method is applicable for s values ranging below about 10–100.

ACKNOWLEDGMENTS

One of the authors (S. N. Antani) would like to thank Professor P. K. Kaw of the Physical Research Laboratory, Ahmedabad, India, Professor J. B. Keller of the Department of Mathematics, Stanford University, Dr. P. Guzdar of the Plasma Group at the University of Maryland, and D. S. Wang of the McDonnell Douglas Corporation, for many helpful suggestions.

This research was supported in part by the Office of Naval Research Contract No. N00014-76-C-0867, National Science Foundation Contract No. MCS-7903498, and AFOSR-82-0154.

[1]B. G. Fejer and M. C. Kelley, Rev. Geophys. Space Phys. **18**, 401 (1980).

[2]C. M. Surko and R. E. Slusher, Phys. Rev. Lett. **37**, 1747 (1976); R. E. Slusher and C. M. Surko, *ibid.* **40**, 400 (1978).

[3]E Mazzucato, Phys. Fluids **21**, 1063 (1978).

[4]K. G. Budden, J. Res. Natl. Bur. Stand. Sect. D **63**, 135 (1959).

[5]D. M. Simonich and K. C. Yeh, Radio Sci. **7**, 291 (1972).

[6]E. Ott, Phys. Fluids **22**, 1732 (1979).

[7]B. Hui, E. Ott, P. T. Bonoli, and P. N. Guzdar, Nucl. Fusion **21**, 339 (1981).

[8]R. A. Helliwell, *Whistlers and Related Ionospheric Phenomena* (Stanford U. P., Stanford, CA, 1965).

[9]K. Theilhaber and A. Bers, Nucl. Fusion **20**, 547 (1980).

[10]S. N. Antani and D. J. Kaup, Phys. Fluids **24**, 1391 (1981).

[11]J. B. Keller, in *Proceedings of the Symposium on Turbulence in Fluids and Plasmas*, Microwave Research Institute's Symposia Series, Vol. 18 (Wiley, New York 1969), p. 131.

[12]C. H. Liu, J. Math. Phys. **8**, 2236 (1967).

[13]Y. Satya and G. Schmidt (private communication).

[14]S. D. Shawhan, *Solar System Plasma Physics*, edited by L. J. Lanzerotti, C. F. Kennel, and E. H. Parker (North-Holland, Amsterdam, 1979), Vol. III, p. 213.

[15]M. Abramovitz and L. Stegun, *Handbook of Mathematical Functions* (National Bureau of Standards, Washington, D. C., 1972).

[16]P. K. Shukla and S. Bujarbarua, J. Geophys. Res. **85**, 1773 (1980).

[17]A. C. Newell, Lect. Appl. Math. **15**, 157 (1974).

[18]P. M. Morse and H. Feshbach, *Methods of Theoretical Physics* (McGraw-Hill, New York, 1953), Vol. I, p. 198.